Seawater signatures of Ordovician climate and environment

Seth A. Young[1]*, Cole T. Edwards[2], Leho Ainsaar[3], Anders Lindskog[4] and Matthew R. Saltzman[5]

[1]Department of Earth, Ocean and Atmospheric Science – National High Magnetic Field Laboratory, Florida State University, Tallahassee, FL 32306, USA

[2]Department of Geological and Environmental Sciences, Appalachian State University, Boone, NC 28608, USA

[3]Department of Geology, University of Tartu, Ravila 14a, Tartu 50411, Estonia

[4]Department of Geology, Lund University, Sölvegatan 12, SE-22362 Lund, Sweden

[5]School of Earth Sciences, The Ohio State University, Columbus, OH 43210, USA

SAY, 0000-0001-6885-4780; AL, 0000-0001-7281-6840
*Correspondence: sayoung2@fsu.edu

Abstract: Tracking climatic changes throughout the Ordovician is crucial to a better understanding of the coevolution of life and environment on Earth. Ordovician climate fluctuations have been the subject of a vigorous and productive body of work over the past two decades. Here we present a synthesis of studies that have focused on reconstructing Ordovician climate and environment via direct geochemical proxy datasets and/or numerical modelling approaches. Many new insights have been gained on potential causes of events: the timing and potential causes of the major radiation of Ordovician marine life, changes in weathering and the transition from a greenhouse-to-icehouse state, and cooling and (de)oxygenation during the end-Ordovician Glaciation. Marked improvements in sample resolution/distribution of traditional palaeotemperature (oxygen isotopes), palaeoredox (sulfur isotopes) and weathering proxy records (strontium and neodymium isotopes), as well as the development of new palaeoenvironmental proxies (e.g. clumped, uranium, molybdenum and thallium isotopes; iodine, iron, trace metal geochemistry), have led to better constraints on Ordovician climate and environment. These recent works have led to a more nuanced understanding of the Ordovician Earth System, which allows the global community to focus future efforts on answering remaining questions regarding palaeoclimate and environment, as well as embark upon new investigations.

The Ordovician Period was long considered a greenhouse state that ended with an anomalous and short-lived Late Ordovician–early Silurian glaciation of the southern portions of the supercontinent Gondwana (Azmy *et al.* 1998; Veizer *et al.* 1999, 2000; Shields *et al.* 2003). The atmospheric partial pressure of carbon dioxide (pCO_2) was generally thought to have been much (*c.* 8–20 times) higher than present atmospheric levels (PAL = 280 ppmv) compared with recent preindustrial atmospheric levels (Berner 1990; Yapp and Poths 1996). This higher CO_2 level was probably counter-balanced in part by lower solar luminosity during the early Phanerozoic (Berner 2006). The partial pressure of oxygen (pO_2) was thought to have been significantly lower (e.g. *c.* 10–15% O_2) in the Ordovician ocean–atmosphere system (Berner 2001). Pioneering numerical climate models attempted to reconcile these very high CO_2 levels with glaciation during the Late Ordovician via unique palaeogeography, palaeotopography and ice–snow albedo feedbacks (Crowley and Baum 1995; Poussart *et al.* 1999). Subsequent studies have presented a contrasting view of Ordovician climate states, indicating that pCO_2 levels were probably on the lower end of the estimated ranges previously proposed and that global ocean heat transport mechanisms were important for ice-sheet initiation for the Late Ordovician (Rothman 2002; Herrmann *et al.* 2003, 2004; Berner 2006; Pancost *et al.* 2013). Additionally, a recent study indicates that ocean temperatures reached modern equatorial ranges during the Middle Ordovician (Barney and Grossman 2022; Edwards *et al.* 2022). Based on both palaeoclimate models and new palaeotemperature proxy data, it appears that Ordovician icehouse conditions were probably long lived (e.g. Saltzman and Young 2005; Pohl *et al.* 2016; Rasmussen *et al.* 2016; Edwards *et al.* 2022). Within this dynamic palaeoclimate backdrop, an unprecedented radiation of marine life occurred (the Great Ordovician Biodiversification Event, GOBE) that was subsequently followed by the first major mass extinction in the Phanerozoic (the Late Ordovician Mass Extinction, LOME; Jablonski 1991). There have

From: Harper, D. A. T., Lefebvre, B., Percival, I. G. and Servais, T. (eds) *A Global Synthesis of the Ordovician System: Part 1*. Geological Society, London, Special Publications, **532**,
https://doi.org/10.1144/SP532-2022-258

been numerous causal linkages proposed for these major biotic events and Earth system climate and environmental changes.

It has been proposed that the GOBE occurred in response to cooling climatic conditions, oxygenation, tectonics, fluctuating sea-level and meteorite impacts (Schmitz *et al.* 2008; Trotter *et al.* 2008; Rasmussen *et al.* 2016; Edwards *et al.* 2017; Stigall *et al.* 2019; Servais *et al.* 2021). The global biodiversity crisis at the end of the Ordovician coincided with the glaciation of polar Gondwana (*c.* modern-day north Africa, Middle East and South America) and a major perturbation of the global carbon cycle (Brenchley *et al.* 1994). Traditionally it has been argued that the LOME was caused by the combined effects of climatic cooling and sea-level fall, as this is the only known major mass extinction that coincides with a glacial episode (Sheehan 2001; Brenchley *et al.* 2003; Finnegan *et al.* 2011). Contrastingly others have linked the LOME to widespread volcanism, climatic warming and/or marine reducing conditions (Hammarlund *et al.* 2012; Jones *et al.* 2017; Bond and Grasby 2020; Dahl *et al.* 2021). Linkages have been proposed between these climatic and environmental changes and increased arc-related orogenesis through the feedbacks associated with silicate weathering and/or volcanic outgassing on pCO_2 levels (Young *et al.* 2009; McKenzie *et al.* 2016; Swanson-Hysell and Macdonald 2017). Additional long-term carbon and oxygen cycle feedbacks have been used to argue for the link between various Ordovician climatic and environmental change events through feedbacks associated with enhanced organic carbon burial and the expansion of marine reducing conditions (i.e. anoxia, euxinia–anoxia plus free hydrogen sulfide) (Kump *et al.* 1999; Brenchley *et al.* 2003; Saltzman and Young 2005; LaPorte *et al.* 2009; Young *et al.* 2010; Hammarlund *et al.* 2012; Thompson and Kah 2012; Edwards *et al.* 2018; Zou *et al.* 2018; Dahl *et al.* 2021; Kozik *et al.* 2022*a*, *b*). Despite more recent and comprehensive approaches that incorporate both physical and geochemical evidence, it remains challenging – and probably/perhaps unrealistic – to single out any one environmental or climatic factor that would completely explain these multifaceted biotic events in the Ordovician (i.e. the GOBE and LOME).

Significant progress has been made in efforts to generate proxy datasets for ancient climate, continental weathering and atmospheric CO_2 and O_2 levels throughout the Ordovician (see chapter subsections below). Reliable proxy records are essential to testing hypotheses involving the co-evolution of tectonics, ocean–atmosphere and life during the Ordovician. Palaeotemperature proxy datasets (e.g. $\delta^{18}O_{brach,}$ $\delta^{18}O_{carb}$, $\delta^{18}O_{phos}$, Δ_{47}) throughout the Ordovician have become more numerous and comprehensive in their coverage over the entire time period (e.g. Trotter *et al.* 2008; Rasmussen *et al.* 2016; Song *et al.* 2019; Goldberg *et al.* 2021; Männik *et al.* 2021; Grossman and Joachimski 2022). These temperature proxy datasets all show a major decline (*c.* 15°C) in estimated sea-surface temperatures (SSTs) from the Early to Late Ordovician, presumably recording the greenhouse-to-icehouse transition (Rasmussen *et al.* 2016). This is broadly consistent with more recent Ordovician climate numerical model simulations that present a possible Middle Ordovician onset of Gondwanan glaciation (Pohl *et al.* 2016). While first-order palaeotemperature trends are emergent at the epoch level within the Ordovician, the magnitude, timing of cooling into modern SST ranges and accurate estimates of palaeotemperatures still remain poorly constrained (e.g. Edwards *et al.* 2022). It has been proposed that rising O_2 levels had a fundamental effect on marine biodiversity during the Ordovician, but poor spatiotemporal resolution and limited redox (reduction–oxidation) proxy data within the Early–Middle Ordovician have hampered detailed interpretations (Thompson and Kah 2012; Young *et al.* 2016; Edwards *et al.* 2017, 2018). Oxygen contents in the ocean–atmosphere system were probably relatively low for most of the early Paleozoic, but there are fundamental disagreements between empirical proxy data and biogeochemical models, as well as differences between models (Krause *et al.* 2018; Tostevin and Mills 2020; Brand *et al.* 2021). Recent ecophysiological–Earth system models incorporating metabolic index have shown that surface oxygenation exhibits first-order controls on extinction rates during the Phanerozoic (Stockey *et al.* 2021). Furthermore, the LOME interval and Hirnantian Stage have been the subject of numerous studies focused on linking palaeoclimate, palaeoceanography and palaeoredox ($\delta^{34}S$, $\delta^{238}U$, $\delta^{98}Mo$, I/Ca ratios) dynamics to biotic turnover events. Yet this level of focus and detailed understanding of palaeoenvironmental conditions has to-date not been achieved within any other stage of the Ordovician Period. The aim of this chapter is to summarize the recent advances in our understanding of geochemical signatures of Ordovician climate and environment. Specifically, we aim to synthesize studies that have focused on reconstructing Ordovician climate and environment via direct geochemical proxy datasets and/or biogeochemical models.

Marine and atmospheric oxygen

A fundamental change in global ocean redox state probably occurred during the Ordovician, as a transition from more pervasive anoxic conditions throughout much of the late Cambrian (Gill *et al.* 2011;

Saltzman *et al.* 2011, 2015) to marine environments that contained oxygen levels high enough to sufficiently support a rapid diversification of benthic marine life during the peak of the GOBE by the Middle–Late Ordovician. Evidence for widespread oceanic anoxia and euxinia during the late Cambrian and Early Ordovician is primarily based on global positive carbon isotopic excursions (CIEs) that have been paired with traditional global redox proxies (e.g. sulfur isotopes: $\delta^{34}S_{CAS}$–carbonate-associated sulfate; Gill *et al.* 2011; Saltzman *et al.* 2015; Edwards *et al.* 2018, 2019; Edwards 2019). A multitude of direct palaeoredox proxies have been developed over the last decade in attempts to better characterize, quantify and understand the significant changes in oxygen levels throughout Earth's history. These novel palaeoredox proxies range from local (e.g. I/Ca ratios, Fe speciation) to global (e.g. δ^{238}U, δ^{98}Mo, ε^{205}Tl) in their extent to fingerprint palaeoredox conditions (e.g. Owens 2019 and references therein). For example, the I/Ca proxy provides an indication of localized water column anoxia when I/Ca values are low in carbonate successions. Importantly, the more recently developed palaeoredox proxies respond to parts of the sequence of biogeochemical reactions/processes that follow oxygen reduction and these are important for marine organisms that can use various alternative electron accepters to create metabolic energy (Froelich *et al.* 1979).

Covariant positive δ^{13}C and δ^{34}S excursions in Phanerozoic marine records are interpreted to have been caused by elevated burial rates of organic carbon and pyrite, respectively, from the global oceans (e.g. Edwards *et al.* 2018). Supporting evidence for this palaeoredox interpretation is documented in the Lower Ordovician successions (Fig. 1 – sulfur isotope panel) and is supported by the fact that trilobite extinction events (biomeres) and other faunas are closely associated with these events (Saltzman *et al.* 2015; Edwards *et al.* 2018, Stockey *et al.* 2021). Furthermore, I/Ca ratios also indicate that local marine anoxia occurred during a Tremadocian coupled positive CIE/extinction event, supporting the notion of the expansion of bottom water anoxic conditions into nearshore environments (Edwards *et al.* 2018).

By the Middle Ordovician (Darriwilian Stage) a clear coupling of positive δ^{13}C and $\delta^{34}S_{CAS}$ excursions appears to have diminished (Young *et al.* 2016), suggesting that marine environments globally had become more oxygenated and therefore the areal extent of bottom water reducing conditions declined (Edwards 2019). Recent modelling approaches suggest that there was a major increase in atmospheric O_2 to near-modern levels that began during the Darriwilian (Fig. 1 – O_2 panel; Edwards *et al.* 2017), which may explain the decrease in magnitude and frequency of paired positive δ^{13}C and δ^{34}S excursions. However, other modelling studies suggest that full oxygenation of the oceans may not have occurred until the Devonian (Krause *et al.* 2018; Lenton *et al.* 2018). The GEOCARBSULFOR model (e.g. Krause *et al.* 2018) utilizes carbon and sulfur isotopic records to produce long-term atmospheric O_2 models and recent simulations show a Late Ordovician rise from 5 to 10%. Similarly, the COPSE model (Lenton *et al.* 2018) does suggest an increase in atmospheric O_2 levels, but the increase only estimates that atmospheric O_2 levels increased from 5 to 12% (% of the atmosphere) by the end-Ordovician. The COPSE model incorporates different kinds of data (e.g. isotopic) from the literature and assumptions about baseline fluxes to the ocean reservoir (e.g. land plant evolution effects on weathering rates), as well as which processes are more important than others with respect to regulating the redox state of the ocean–atmosphere system. Thus, it is understandable and expected that there is some discrepancy between these numerical modelling approaches, particularly when taking into account differences in which rocks were sampled to generate geochemical data and what environments those strata represent (e.g. epeiric-sea carbonates, deep-distal marginal fine-grained siliciclastics). Alternatively, recent Earth system model experiments indicate a potential role for changing palaeogeography in marine oxygenation (Pohl *et al.* 2022). Specifically, these model simulations produce fundamental decoupling of subsurface and deep ocean O_2 levels and present new challenges to how global marine redox proxies can be used in other biogeochemical box models to infer pO_2 (Pohl *et al.* 2021, 2022).

While atmospheric O_2 models show some discrepancies, other geochemical proxies that assess ocean redox state also suggest that oxygenation occurred during the Ordovician. For example, Mo isotopes (δ^{98}Mo), which reflect the global ocean δ^{98}Mo value owing to its long residence time (>800 kyr), show an increasing trend from values typical of reducing conditions during Early Ordovician to more oxidizing conditions by the end of the Period (Dahl *et al.* 2010). Furthermore, the concentrations of U and Mo in Ordovician organic-rich shales (normalized to total organic carbon) show that more oxidizing conditions were reached by the Middle Ordovician (Hennessy and Mossman 1996; Schovsbo 2002; Abanda and Hannigan 2006). Still, trace metal concentrations from organic-rich shales (as many other types of redox proxies) are not necessarily global indicators of reducing–oxidizing conditions as they can also be affected by basin connectivity to the open ocean and changes in local redox conditions as well as changes to global trace metal inventories (Algeo and Lyons 2006; Lyons *et al.* 2009).

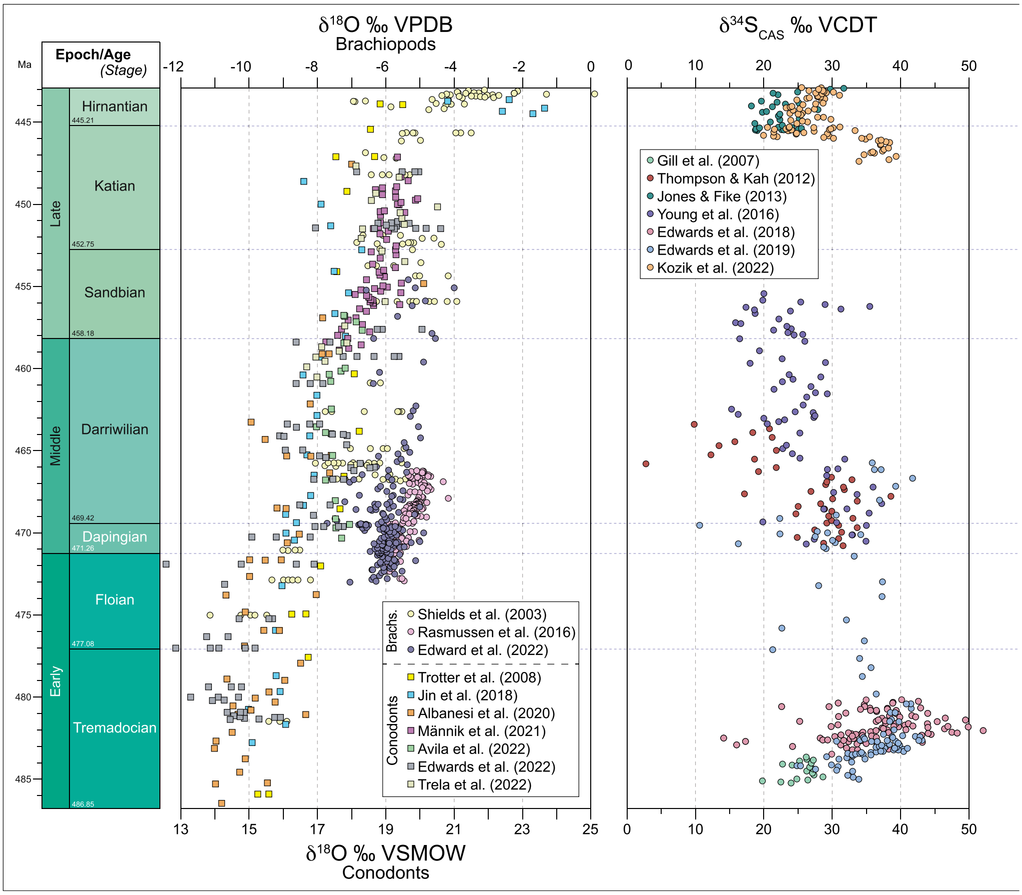

Fig. 1. Compilation of palaeoenvironmentally significant data in the Ordovician, based on a selection of representative and stratigraphically comprehensive datasets at the global scale. Carbon dioxide (CO_2) curves according to Cocks and Torsvik (2021, dotted line) and Conwell *et al.* (2022, solid line). Oxygen (O_2) according to Edwards *et al.* (2017, solid line) and Krause *et al.* (2018, dotted line). Sea-surface temperature (SST) curve according to Goldberg *et al.* (2021; lowest SST decile, i.e. highest δ^{18}O decile). Ice extent estimated based on Ghienne *et al.* (2007), Kumpulainen (2007), Loi *et al.* (2010), Goldberg *et al.* (2021) and Rasmussen *et al.* (2021).

Although the collective data suggest that there was a first-order increase in oxygen levels throughout the Ordovician, the redox state of the global ocean appears to have been more dynamic; significant shifts to more widespread reducing conditions (anoxia to euxinia) appear to have occurred in some time intervals. One possible example of dynamic fluctuations in marine redox conditions (e.g. intermittent anoxia–euxinia) probably occurred during the end-Ordovician. Owing to the coincidence of the first major mass extinction in the Phanerozoic, the LOME, large-scale Gondwana glaciation and one of the largest globally correlative positive δ^{13}C excursions (HICEs), the Hirnantian Stage has become the most well-studied interval of the Ordovician with regards to palaeoredox and palaeoclimate (Kump *et al.* 1999; Sheehan 2001; Young *et al.* 2010; Harper *et al.* 2014; Jones *et al.* 2016). Although icehouse conditions are widely thought to promote more vigorous global thermohaline circulation, delivering cool and oxygenated surface waters to the deep ocean (Pohl *et al.* 2017), this appears to be at odds with several recent studies that have documented widespread anoxic to euxinic conditions during certain intervals within the Hirnantian (Zou *et al.* 2018). To further complicate this picture, records of marine sulfur cycling seem to have some inconsistencies as there is a large positive δ^{34}S excursion in the Hirnantian pyrite records from multiple palaeocontinents (Zhang *et al.* 2009; Gorjan *et al.* 2012; Hammarlund *et al.* 2012; Yan *et al.* 2012; Young *et al.* 2020), but there is almost no

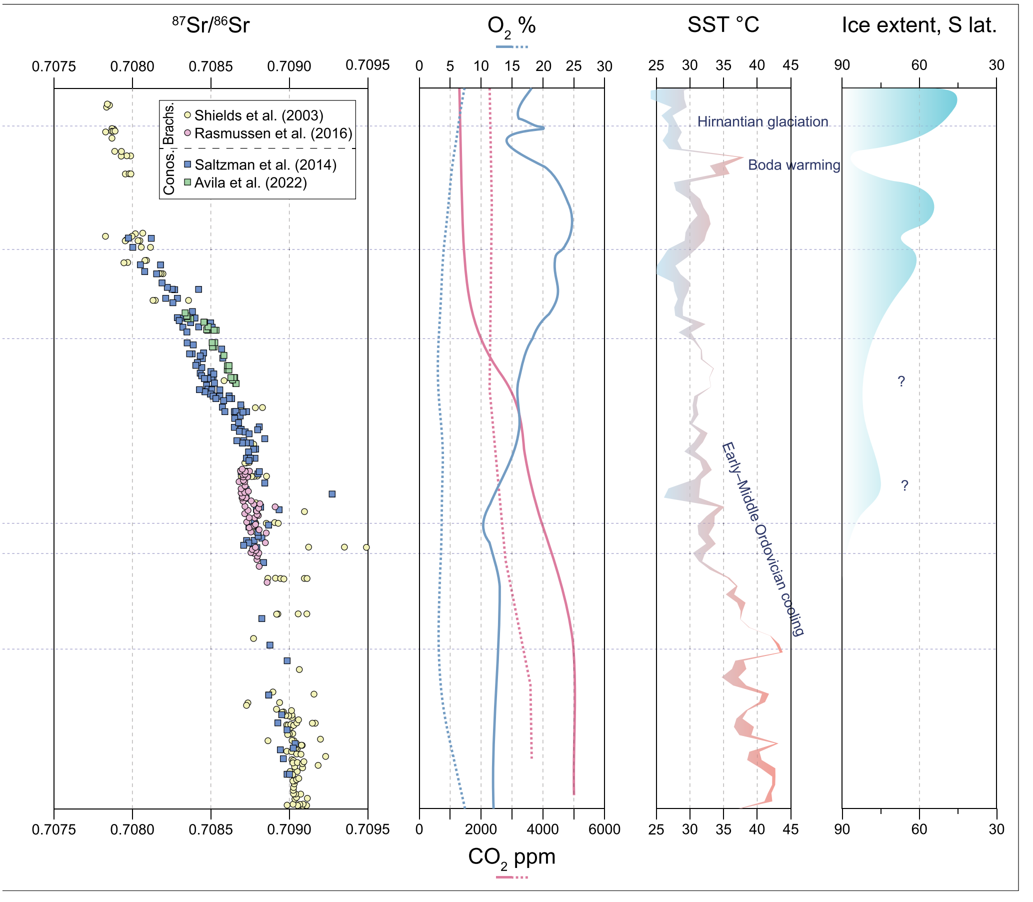

Fig. 1. Continued

change in the seawater sulfate ($\delta^{34}S_{CAS}$) proxy record (Jones and Fike 2013). Other evidence for global anoxia comes in the form of uranium isotopes ($\delta^{238}U$) where $\delta^{238}U$ values decrease at the end of the Hirnantian Stage, similar to other times in Earth history where evidence of anoxia is present (Bartlett *et al.* 2018). Lastly, localized anoxia also appears to have persisted for part of the Hirnantian, if not its entirity, based on I/Ca records from multiple shallow platform carbonates (Kozik *et al.* 2022*a*). These recent palaeoredox proxies throughout the Hirnantian broadly support the results of metazoan ecophysiological models that indicate that large magnitude extinction events during the early Paleozoic (e.g. LOME) were a consequence of limited surface oxygenation and temperature-dependent hypoxia responses (Stockey *et al.* 2021). Despite these complexities that are present in the Hirnantian palaeoredox proxies, more recent integrated approaches to Hirnantian sea-level, climate, mass extinction and (de)oxygenation are beginning to emerge (see the Hirnantian glaciation and mass extinction section below for further details).

In summation, modelling and geochemical evidence indicate that there were significant changes to the redox state of the global oceans during the Ordovician. Thus far the local and global palaeoredox proxy studies of the Early Ordovician are few but those studies point towards at least one major interval of widespread marine anoxic (possibly euxinic) conditions in the Tremadocian. This supports the hypothesis that the Early Ordovician was not yet hospitable to marine life compared with the Late Ordovician (e.g. Saltzman *et al.* 2015). The late Early through Middle Ordovician experienced a significant increase in marine diversity, which may have been facilitated by an increase in oxygenated waters to expand habitable environments on the seafloor. This is apparently also indicated by a successive increase in the relative proportion of skeletal grains in sedimentary rocks (e.g. Lindström 1979; Pruss *et al.* 2010; Lindskog and Eriksson 2017). It remains unclear, however, exactly how much oxygen was present in the Ordovician atmosphere (Edwards *et al.* 2017; Krause *et al.* 2018; Lenton *et al.* 2018). The causes of progressive atmospheric oxygenation in the Ordovician have not yet been resolved, but could reflect continued and markedly increased photosynthesis in the oceans and newly evolved terrestrial-based primary producers (Lenton *et al.* 2016). Alternatively, or in addition, Ordovician marine oxygenation could have been facilitated by continued cooling of the climate owing to changes in silicate weathering/volcanic degassing (Nardin *et al.* 2011; Conwell *et al.* 2022; Edwards *et al.* 2022). It should be noted that a large majority of the Ordovician lacks any detailed palaeoredox proxy-based studies, with our most detailed understanding of oxygen contents coming from the mid-Tremadocian, Darriwilian and Hirnantian intervals. Thus, it is clear that more detailed proxy-based palaeoredox studies are needed to grasp a detailed first-order view of the redox dynamics of the Ordovician ocean–atmosphere system.

Palaeotemperature and oxygen isotope methodology

Stable oxygen isotopes ($\delta^{18}O$) are used to estimate palaeotemperatures of Ordovician seas from a variety of minerals and fossils. These include low-Mg calcite from brachiopod shells (Veizer *et al.* 1999; Shields *et al.* 2003; Rasmussen *et al.* 2016; Bergmann *et al.* 2018), conodont apatite (Trotter *et al.* 2008; Quinton *et al.* 2018*a*, *b*; Albanesi *et al.* 2020; Edwards *et al.* 2022) and clumped $\delta^{18}O$ isotopes (Finnegan *et al.* 2011, 2012; Bergmann *et al.* 2018). Together, these isotope proxies indicate that Ordovician oceans cooled from seemingly especially warm temperatures (>40°C; Shields *et al.* 2003; Trotter *et al.* 2008) during the earliest Ordovician to moderate temperatures during the Floian to Katian stages, and reached the coolest temperatures during the Hirnantian, coinciding with maximum ice-sheet advance (Fig. 1 – SST panel). However, all proxies have their own caveats and any inherent information about the Ordovician world is somewhat limited as diagenetic overprints have obscured many of the primary seawater signatures from this time.

Brachiopod calcite is regarded by many as an ideal mineral to sample for $\delta^{18}O$ values to reconstruct palaeotemperatures, as long as the $\delta^{18}O$ value of seawater can be assumed (e.g. Veizer *et al.* 1999). These minerals are easy and inexpensive to analyse in most geochemistry laboratories equipped with a mass spectrometer capable of measuring CO_2 gas. Not only is this form of calcite (low-Mg calcite) the most resistant to alteration and re-equilibration with seawater or pore fluids, but recrystallization of the targeted calcitic prismatic layer can be verified with scanning electron and cathodoluminescent microscopy (Veizer *et al.* 1999; Shields *et al.* 2003). Furthermore, screening of diagenetically affected brachiopods using trace element compositions (Mn and Sr concentrations) can be used to prevent unnecessary analysis of $\delta^{18}O$ values from these brachiopods. However, brachiopod-based approaches include limitations, such as suitable fossil availability in a particular section. Not all carbonate successions contain brachiopod-bearing facies appropriate for isotopic study, so some intervals in time cannot be sampled for this style of palaeotemperature reconstruction. Screening for alteration is also time consuming if each fossil is imaged using microscopy techniques and screened for trace element compositions. A compilation of $\delta^{18}O$ data from well-preserved brachiopods shows that Ordovician oceans cooled from the Tremadocian to Darriwilian (Fig. 1 – oxygen isotope panel; Shields *et al.* 2003), but conversion of $\delta^{18}O$ values to palaeotemperatures using the equation of Kim and O'Neil (1997) indicates that Tremadocian oceans were unrealistically warm (40–70°C) if seawater $\delta^{18}O$ was *c.* −1‰. It may be possible that seawater $\delta^{18}O$ values varied outside of the −1–0‰ range we observe between modern glacial–interglacial cycles (Wallmann 2001; Shields *et al.* 2003; Jaffrés *et al.* 2007; Veizer and Prokoph 2015), but it is also likely that some $\delta^{18}O$ values have been altered during burial diagenesis despite samples passing the aforementioned screening criteria (cf. Bergmann *et al.* 2018).

Another fossil mineral that is commonly used to reconstruct Ordovician palaeotemperatures is apatite. Apatite, or bioapatite, can be in the form of bone, fish scales, phosphorite or conodont apatite, but only conodont apatite is used to reconstruct Ordovician palaeotemperatures as the first two have essentially no Ordovician fossil record, and phosphorites have poor age resolution compared with conodonts. Phosphate minerals are thought to be excellent records of seawater $\delta^{18}O$ (i.e. palaeotemperature) during the time of biomineralization because the strong P–O bonds are resistant to thermal alteration during burial diagenesis (e.g. Kolodny *et al.* 1983; Shemesh *et al.* 1983). Conodont apatite, known as the mineral francolite (Pietzner *et al.* 1968), can offer superior age resolution of palaeotemperature estimates as many Ordovician successions contain sufficient conodont apatite material to analyse. The two methods used to measure the $\delta^{18}O$ value of conodont apatite are (1) measuring a purified $AgPO_4$ precipitate, commonly from dozens of elements, in a high-temperature conversion elemental analyser (TC/EA), or (2) measuring *in situ* analysis of individual elements in either a secondary ion mass spectrometer (SIMS) or sensitive high-resolution ion microprobe (SHRIMP; e.g. Trotter *et al.* 2008; Edwards *et al.* 2022). The δ^{18}O values can be converted to palaeotemperatures using several empirically derived equations (Longinelli and Nuti 1973; Kolodny *et al.* 1983; Pucéat *et al.* 2010). The following equation was developed by Lécuyer *et al.* (2013), and is the most recent:

$$T(^{\circ}\mathrm{C}) = 117.4(\pm 9.5)\text{–}4.50(\pm 0.43) \times (\delta^{18}\mathrm{O}_{\mathrm{conodont}}\text{–}\delta^{18}\mathrm{O}_{\mathrm{seawater}})$$

Both methods used to generate δ^{18}O values have their own limitations that should be considered when making palaeotemperature estimates, particularly considering uncertainty alone in the above equation. Moreover, the methods are sample-destructive, and one of the downsides to using the TC/EA method is that dozens of conodont elements are needed, depending on their sizes, in order to generate enough $AgPO_4$ precipitate for analysis (Quinton and MacLeod 2014). The SIMS or SHRIMP approaches, however, can analyse a single element, many times, to decrease analytical uncertainty. These approaches can also target specific conodont tissues (i.e. albid v. hyaline crown material) to avoid tissues thought to be more susceptible to alteration or exchange during burial diagenesis (Trotter and Eggins 2006; Wheeley *et al.* 2012; Zhang *et al.* 2017). However, one advantage to using the TC/EA method is that the conodont apatite is purified using ion chromatography, where the only oxygen phase measured is that of the PO_4 itself. SIMS and SHRIMP methods instead analyse all apatite material, which can include up to 10% stoichiometric non-PO_4 oxygen as either CO_3 or OH (Pietzner *et al.* 1968). As such, SIMS/SHRIMP-generated δ^{18}O data should be corrected when compared with TC/EA-generated δ^{18}O values as the latter come from pure PO_4 and should theoretically record palaeotemperatures. Comparisons of conodont apatite using both methods have shown that SIMS/SHRIMP-generated δ^{18}O data are 1–1.5‰ more positive than TC/EA-generated δ^{18}O values (Trotter *et al.* 2015; Edwards *et al.* 2022). One potentially important implication of this needed correction is that cooling of Ordovician seas to modern SSTs by the Darriwilian (Trotter *et al.* 2008) may not have progressed by enough to match modern temperatures as oceans would still have been too warm for most marine invertebrates. A 1–1.5‰ correction adds 4.5–6.8°C to palaeotemperature estimates using the equation above (this translates to 35–38°C for the Darriwilian), which seems unreasonably warm and above the thermal tolerance of many marine genera, yet this was during the Great Ordovician Biodiversification Event (Rasmussen *et al.* 2016; Stigall *et al.* 2019). Instead, it is more likely that either the empirically derived equations used to calculate palaeotemperatures using bioapatite δ^{18}O values are not appropriate for conodont apatite and/or that seawater δ^{18}O values were not at a constant value of *c.* −1‰ during this time, although Bergmann *et al.* (2018) suggest that seawater δ^{18}O remained relatively constant near −1‰ during the Cambrian–Ordovician. Palaeotemperature estimates generated using means independent of having to assume the δ^{18}O value of seawater will help to resolve this uncertainty. Lastly, temperature estimates may be distorted based on latitudinal sampling biases where over/under-sampling in the tropics, for example, may not truly capture a global signal if only samples from the tropics are sampled (e.g. Jones and Eichenseer 2022). A more even latitudinal sampling of δ^{18}O estimates should help to minimize methodology artefacts and create a clearer view of Ordovician temperature trends.

The carbonate clumped isotope palaeothermometer is another method of estimating palaeotemperatures based on the temperature-dependent relationship between ^{13}C and ^{18}O isotopes in carbonate-bearing minerals, which is independent from the δ^{18}O value of seawater (Came *et al.* 2007). The clumped isotope proxy has been used to estimate seawater temperatures during the Late Ordovician Hirnantian glaciation (Finnegan *et al.* 2011, 2012), and of the Cambrian–Ordovician (Bergmann *et al.* 2018). During the Hirnantian, tropical SSTs are thought to have dropped by 5°C, which coincides with evidence of extensive land-ice development (Ghienne *et al.* 2007; Finnegan *et al.* 2011). During the Middle Ordovician, clumped isotopes suggest temperatures that were probably similar or slightly warmer compared with modern seas (Bergmann *et al.* 2018). These clumped isotopic estimates find no evidence for a steady cooling from the Late Cambrian to Middle Ordovician (Fig. 1), but the existing sample resolution is too poor to conclusively rule this cooling out. Although this palaeotemperature method is ideal to use compared with δ^{18}O-based palaeotemperature estimates from carbonate or apatite because it does not require independent knowledge of the seawater δ^{18}O value, it also has its own pitfalls. Perhaps the most serious limitation to this proxy is that diagenetic overprinting or secondary carbonate precipitation can obscure primary seawater signatures. Bergmann *et al.* (2018) report minimum temperature estimates of Ordovician brachiopods, but even some of these estimates exceed 40°C and probably record diagenetic overprinting (despite these fossils physically appearing well preserved using scanning electron microscopy). Another caveat to using this proxy is that the analytical method requires the use of a mass spectrometer equipped with more Faraday cups than what most laboratories have available in their instrument(s). Lastly, the clumped isotope method requires significantly more sample powder than a traditional $\delta^{18}O$ analysis (because the $^{13}C^{18}O^{16}O$ molecule is far less abundant than mass units 44–46). Although this normally is not a problem for large-shelled brachiopods (more common in Upper Ordovician strata), it can be problematic for thin-shelled or small fossils.

Ideally, because phosphate is thought to be more resistant to diagenesis than carbonate minerals (e.g. Shemesh *et al.* 1983), it seems that the clumped isotope proxy should be used to estimate Ordovician palaeotemperatures. However, the two main sources of Ordovician biogenic apatite are inarticulate brachiopods and conodonts, the former of which have been the target of a preliminary study (Bergmann *et al.* 2018). Because conodont apatite does contain trace amounts of carbonate (0.36 wt%; Pietzner *et al.* 1968), theoretically it could be used for clumped isotopic study. However, this kind of analysis would require a significant amount of conodont material to generate meaningful data, particularly if replicate samples were to be run. Hopefully future studies of clumped isotopes focused on reconstructing Ordovician palaeotemperatures can involve collaboration with those with extensive conodont collections to pursue this potentially major advance in better understanding the Ordovician climate.

Ordovician cooling: greenhouse-to-icehouse transition

The timing of the Ordovician greenhouse to icehouse transition can be considered from the perspectives of the physical evidence for ice sheets, which can include tillites (near-field) or other features (e.g. Ghienne *et al.* 2007) and eustatic sea-level changes (far-field) and isotopic evidence for cooling or ice build-up in the form of oxygen isotope records. More indirectly, isotope proxy records of changes in the sources and sinks of atmospheric CO_2, primarily carbon and strontium isotopes, may be linked to changes in palaeoclimate.

Ghienne *et al.* (2007) summarized the Late Ordovician glacial sedimentary system of the high-latitude Gondwanan regions, which revealed unambiguous evidence for glaciation in the form of tillites at the end of the Ordovician. Prior to these tillite deposits, there is no unambiguous evidence for glaciation. More indirectly, Dabard *et al.* (2015) looked at Middle to Late Ordovician sea-level curves in the Armorican Massif (western France) and concluded that there was evidence for glacio-eustasy throughout this time period. Dabard *et al.* (2015) used a sequence stratigraphic approach, combining facies and parasequence stacking patterns, together with gamma-ray analysis within a chitinozoan-based biostratigraphic framework. Seven sea-level falls of about 50–80 m were identified on time scales of less than 100 kyr during the Darriwilian and the Sandbian. Rasmussen *et al.* (2016) further supported this notion of glacio-eustasy during the Middle Ordovician utilizing pristine brachiopod $\delta^{18}O$ data, and local sea-level curves from Baltica.

The $\delta^{18}O$ record of the Ordovician is coming into focus, but the challenge of separating temperature and ice volume makes it difficult to pinpoint the icehouse transition. The broad first-order structure seems clear, with a substantial increase in $\delta^{18}O$ values from the beginning of the Ordovician to the end (Fig. 1). This trend is corroborated by many studies spanning all or most of the Ordovician, cited in the above section on $\delta^{18}O$, notably including Shields *et al.* (2003, brachiopods), Trotter *et al.* (2008, conodonts) and Edwards *et al.* (2022), who compiled new and published Ordovician conodont-based data based on using SIMS analyses. Goldberg *et al.* (2021) looked at the entire Ordovician and showed that, despite susceptibility to diagenetic alteration, bulk carbonate $\delta^{18}O$ apparently record this first-order cooling (along with the higher frequency structure; see also Lindskog *et al.* 2019; Edward *et al.* 2022; and references therein). More recently Grossman and Joachimski (2022) reassessed ocean temperatures throughout the Ordovician. These authors suggest that average low-latitude (30°S to 30°N) palaeotemperatures for shallow environments declined from 42.0 $\pm$ 3.1°C during the Early–Middle Ordovician to 35.6 $\pm$ 2.4°C for the Late Ordovician. Importantly, the conodont $\delta^{18}O$ record aligns well with brachiopod calcite. Barney and Grossman (2022) examined clumped isotope studies and determined that typical subtropical surface waters may have been as warm as 35°C approaching the Hirnantian glaciation. They further state that 'temperatures remained warm immediately prior to and perhaps during the transition to the Hirnantian glaciation'.

The second-order structure of the Ordovician $\delta^{18}O$ curve is also starting to reveal some reproducible trends between widely separate regions, which could potentially signal cooling events and/or ice build-up (Fig. 1). Notably, several recent $\delta^{18}O$ publications show that the proposed interval of Taconic basalt weathering (Young *et al.* 2009; Swanson-Hysell and Macdonald 2017) appears to coincide with cooling. The $\delta^{18}O$ dataset from Edwards *et al.* (2022) in the Antelope Range of Nevada can be tied directly to the Sr and Nd isotope data in Conwell *et al.* (2022). $\delta^{18}O$ values from Avila *et al.* (2022) in the Arbuckle Mountains of Oklahoma can also be compared with the Sr isotope curve (Saltzman *et al.* 2014) and the $\delta^{18}O$ values of Edwards *et al.* (2022) with all datasets from the same sections. Männik *et al.* (2021) present $\delta^{18}O$ data from Estonia and also demonstrate that a cooling occurred during the latest Darriwilian through early Sandbian, consistent with Yangtze Platform data published in Jin *et al.* (2018). Liu *et al.* (2022) showed a cooling from China that initiated in the *Pygodus serra* conodont zone and continued through the early Katian. Trela *et al.* (2022) showed data from Poland consistent with a mid-Darriwilian to early Sandbian rise in $\delta^{18}O$. There is some evidence as well for a warming during the early Darriwilian, which precedes this cooling episode, although fewer datasets cover this interval. Edward *et al.* (2022) provided a Baltic perspective on the Early to early Late Ordovician $\delta^{18}O$, which revealed a long-term Lower to Upper Ordovician trend of increasingly more positive brachiopod $\delta^{18}O$ values, with a pronounced cooling during the Early–Middle Ordovician.

As mentioned above, the evidence for changes in carbon cycling that should lead to glaciation mainly come from radiogenic isotope data and associated modelling exercises (Young *et al.* 2009; Avila *et al.* 2022; Conwell *et al.* 2022). Although it remains unclear whether a lower rate of volcanic degassing of CO_2 could drive Ordovician climate towards an icehouse (Marcilly *et al.* 2022), there is evidence for enhancement of the mafic (Ca, Mg-silicate) weathering (CO_2 sink). Conwell *et al.* (2022) presented a uniquely age-constrained and integrated Middle–Late Ordovician (470 – 450 Ma) continental weathering proxy dataset ($^{87}Sr/^{86}Sr$ and $\varepsilon_{Nd(t)}$) from carbonates in the Antelope Range of central Nevada paired with published palaeotemperature proxy measurements ($\delta^{18}O$) of conodont apatite from the same locality (Edwards *et al.* 2022). The Sr and Nd proxy records are consistent with an increase in mafic weathering of the Taconic mountains at *c.* 463 Ma, which forced a period of global cooling. These new palaeotemperature and weathering proxy advancements are broadly consistent with palaeoclimate model simulations that also converge upon Middle–Late Ordovician tipping points in pCO_2 levels induced by palaeogeography and surface area exposures of fresh mafic volcanics (Nardin *et al.* 2011). Furthermore, palaeoclimate models suggest that palaeogeography (predominantly oceanic northern hemisphere), ocean heat transport and modest declines in pCO_2 levels (between 16 and 12 PAL) can generate the build-up of ice sheets as early as the Darriwilian of the Middle Ordovician (Pohl *et al.* 2014, 2016). Recent Ordovician carbon cycle–climate model simulations indicate that even with new Taconic arc weatherability enhancements taken into account (Swanson-Hysell and Macdonald 2017; Macdonald *et al.* 2019), these alone cannot explain Middle–Late Ordovician cooling (Marcilly *et al.* 2022). Based upon these recent Ordovician climate modelling attempts, it is clear that alternative sources (e.g. degassing fluxes) and sinks (i.e. organic-carbon burial, the appearance of non-vascular land plants) need to be explored and constrained further to bring model and proxy data into closer alignment (Marcilly *et al.* 2022).

Our understanding of fluctuations in Ordovician seawater dissolved inorganic carbon isotopic values has been well established over the last several decades through the generation of carbon isotope profiles for Ordovician marine limestones on a global scale. For detailed compilations of Ordovician $\delta^{13}C_{carb}$ records we refer readers to recent efforts within the Geologic Time Scale 2020 (Cramer and Jarvis 2020; Goldman *et al.* 2020). The $\delta^{13}C$ record through the Ordovician reveals substantial variation, some of which can be tied to evidence of cooling and possibly ice build-up (e.g. Saltzman and Young 2005; Ainsaar *et al.* 2010; Rasmussen *et al.* 2016; Lindskog *et al.* 2019; Edward *et al.* 2022). However, there remain new questions about the significance of these carbon isotope variations, and whether they represent changes in the global burial rates of organic carbon (Lindskog *et al.* 2019; Lindskog and Young 2019). With the novel calcium isotope proxy only beginning to be studied in the Ordovician, it is not yet clear whether diagenetic explanations such as that proposed by Jones *et al.* (2020) for the HICE could be applied to other events. Furthermore, the work of Geyman and Maloof (2019) showed that platform carbonate carbon isotope values can evolve separately from the global ocean dissolved inorganic carbon pool. Regardless of the ultimate explanation for the Ordovician $\delta^{13}C$ variability that is observed, a global explanation is suitable in many intervals where distinct variations correlate globally.

Katian cooling to Boda warming?

The Katian–Hirnantian stages of the Late Ordovician represent a time of notably fluctuating climate and global environmental conditions. This assumption is mainly based on palaeontological data and interpretation of sea-level changes, but it can also be seen within the stable isotope geochemistry of sedimentary components. The $\delta^{13}C$ curves of Katian carbonate successions in different basins worldwide include a series of distinct 1–3‰ magnitude positive excursions from baseline values (e.g. Saltzman 2005; Bergström *et al.* 2009*a*; Cramer and Jarvis 2020). The basal Katian Guttenberg Carbon Isotope Excursion (GICE) has been recorded and correlated globally between different palaeocontinents, for example, Laurentia (Bergström *et al.* 2010*a*), Baltica (Ainsaar *et al.* 1999, 2010), Siberia (Ainsaar *et al.* 2015), South America (Sial *et al.* 2013), South China (Bergström *et al.* 2009*b*; Munnecke *et al.* 2011) and the Tarim Basin (Liu *et al.* 2016; Zhang and Munnecke 2016). A number of smaller (1–2‰) positive $\delta^{13}C$ excursions have been documented in between the GICE and HICE in different basins worldwide. In Baltoscandia four excursions have been named as the Rakvere, Saunja, Moe and Paroveja (Ainsaar *et al.* 2010), and in the American midcontinent five excursions are recognized as the Whitewater, Waynesville, Fairview, Kope and Elkhorn excursions (Bergström *et al.* 2010*b*). Bergström *et al.* (2010*b*, 2015, 2020) have proposed the transcontinental correlation between Laurentia and Baltica for these Katian excursions and discussed their global nature. However, the present resolution of the biostratigraphic ties between the sedimentary successions of these palaeocontinents leaves the precise correlation of the smaller positive CIEs still a matter of discussion and active work (Cramer and Jarvis 2020; Goldman *et al.* 2020).

The chemostratigraphic correlation of smaller Katian $\delta^{13}C$ excursions between basins and continents is partly complicated because the stratigraphic positions of the CIEs (i.e. the beginning, peak and termination of the CIE) are sometimes arbitrarily defined and problematic owing to inconsistent sampling resolution between sections. Additionally, facies (or 'aquafacies') differences reflected in $\delta^{13}C_{carb}$ values in Ordovician carbonate depositional environments have been documented (e.g. Holmden *et al.* 1998; Young *et al.* 2005; Panchuk *et al.* 2006; Saltzman and Edwards 2017; Lindskog *et al.* 2019). These trends have, for example, been interpreted as an influence of local input of isotopically light carbon from various sources to the shallow restricted platform (e.g. Saltzman and Edwards 2017) and it could be a potential pitfall in the potential of high-resolution regional–global correlation of these isotopic events.

The GICE interval at the Sandbian–Katian boundary has been considered to mark environmental change from relatively stable warmer conditions to relatively unstable cooler climate (Saltzman 2005) and the beginning of the long-lived Ordovician glaciation (Pope and Steffen 2003; Saltzman and Young 2005). The idea of the GICE as a cooling (or even glacial) episode has been partly based on the analogue with the HICE, as it represents a global positive CIE and coincides with sea-level fall and faunal changes in some basins (e.g. Ainsaar *et al.* 2004). A number of oxygen isotope datasets both from conodont apatite and brachiopod calcite have been published from the Katian (Fig. 1 – oxygen isotope panel), in attempts to estimate the SST variations in various basins (see above for more detail). The classic but relatively low-resolution conodont $\delta^{18}O$ record by Trotter *et al.* (2008), spanning the entire Ordovician period, suggested stable temperatures during the Katian, following a steady cooling trend through the Early and Middle Ordovician. Detailed conodont $\delta^{18}O$ analyses from different sections in Laurentia representing tropical basins (Buggisch *et al.* 2010; Herrmann *et al.* 2010; Rosenau *et al.* 2012; Quinton and MacLeod 2014) have thus far not demonstrated a long-term SST shift through the Katian that is consistent with proposed climate volatility during the Late Ordovician, pre-Hirnantian interval (Goldberg *et al.* 2021).

The question whether the Hirnantian glacial event was preceded by a warming episode during the Katian has repeatedly been discussed over the last few decades (e.g. Melchin *et al.* 2013). The term 'Boda event' was introduced by Fortey and Cocks (2005) to mark the time interval during the Katian when warm-water shelf carbonates and benthic faunas appeared to spread into higher latitude settings (Fig. 1 – SST panel). Subsequently, Cherns and Wheeley (2007) instead interpreted the environmental changes of the Boda event as evidence for global cooling. The rising number of geochemical datasets has been used to discuss the timing and the structure of the climate changes previously taken as the single Boda event (Melchin *et al.* 2013). Finnegan *et al.* (2011) used carbonate clumped isotope palaeothermometry to show Katian–Aeronian SST fluctuations in Laurentia. These changes included the mid-Katian cooling, early Boda warming, mid Boda cooling and late Boda warming immediately before the Hirnantian cooling (event names by Melchin *et al.* 2013). Zhang *et al.* (2021) have analysed the Chemical Index of Alteration of the Late Ordovician siliciclastic sediments in Tarim Basin. These chemical weathering trend data have been interpreted to confirm the cooling and warming cycle, corresponding to the mid-Boda cooling and the late-Boda warming events (Melchin *et al.* 2013; Zhang *et al.* 2021).

Goldberg *et al.* (2021) compiled a massive dataset of the bulk carbonate $\delta^{18}O$ values and analysed this dataset by selecting the lowest deciles of the values by narrow moving age windows to build the secular temperature curve. From this analysis, the aforementioned authors suggested that global warming occurred during the earliest Katian, followed by a return to cooler temperatures before the Hirnantian glaciation (Fig. 1; Goldberg *et al.* 2021). A few detailed studies have attempted to integrate conodont $\delta^{18}O$ values, sedimentary facies and sea-level change in the Katian. Specifically, this has been done in different parts of Laurentia (the midcontinent USA and Anticosti Island; Elrick *et al.* 2013) and in Baltica (Estonia; Männik *et al.* 2021). Considering the synchronous changes in sedimentary facies, conodont populations and early diagenesis (e.g. hardground formation) related to sea-level fall episodes, future work is still needed to understand if and/or how the SSTs fluctuated owing to glaciation cycles during the Katian. Additionally, palaeoclimate modelling does suggest the possibility of Gondwanan ice sheets during the Katian but they may not have been stable on long time-scales owing to overall higher pCO_2 levels than those inferred for the Hirnantian (Pohl *et al.* 2016). The numerous geochemical studies about the Katian climatic changes are still contradictory in-between some details, but generally there is some consensus that the Katian could be seen as prelude to the rapid and dramatic climatic shifts that are well documented at the end of the Ordovician Period (Loi *et al.* 2010).

Hirnantian glaciation and mass extinction

The Late Ordovician represents a significant period of environmental, biotic (LOME) and climatic upheaval, which has been widely studied; the Hirnantian Stage in particular has been extensively investigated. The classical two-pulse mass extinction model with successive survival faunal intervals with connections to glaciation, sea-level, and anoxia has been widely accepted (Sheehan 2001; Brenchley *et al.* 2003; Harper *et al.* 2014), although the LOME has been recently proposed to be just a single-pulse event followed by a prolonged recovery interval (Wang *et al.* 2019). Both the near-field Hirnantian glaciogenic sedimentary records from polar Gondwana and far-field eustatic sea-level records are the subject of more detailed discussion/synthesis elsewhere in this special publication and thus we focus on the geochemical proxy records of climatic and environmental change.

There is mounting geochemical evidence that changes in oxygen contents of marine environments began during the late Katian and were coincident with high sea-level, elevated tropical SSTs and generally high levels of marine biodiversity (Finney *et al.* 1999; Haq and Schutter 2008; Trotter *et al.* 2008; Finnegan *et al.* 2011; Bartlett *et al.* 2018; Dahl *et al.* 2021; Kozik *et al.* 2022*a*, *b*). Evidence from clumped oxygen isotopes and conodont palaeothermometry suggest that average tropical SSTs began declining during the latest Katian (Fig. 1) with the initiation of Gondwanan ice-sheet expansion (Fig. 1; Trotter *et al.* 2008; Loi *et al.* 2010; Finnegan *et al.* 2011; Goldberg *et al.* 2021). Additionally, a large-magnitude positive carbon isotope excursion, the HICE, has been recorded globally in both $\delta^{13}C_{carb}$ and $\delta^{13}C_{org}$ datasets in Hirnantian strata of varying lithologies (e.g. carbonates to organic-rich shales). This positive CIE ranges in magnitude between +4‰ (Anticosti Island, Midcontinent USA, South China, Sweden) and up to +7‰ (Arctic Canada, Nevada USA, Estonia, Norway) (Kump *et al.* 1999; Melchin and Holmden 2006; LaPorte *et al.* 2009; Yan *et al.* 2009; Young *et al.* 2010; Jones and Fike 2013; Hammarlund *et al.* 2012). There have been multiple end-Ordovician glacial–interglacial cycles identified from polar Gondwana glaciogenic sediments as well as low-latitude carbonate platform settings (e.g. Ghienne *et al.* 2007, 2014 and references therein). The connections between Hirnantian $\delta^{13}C$ records, climate and Gondwanan ice-sheet dynamics still remain poorly understood, with linkages ranging from sea-level driven changes in carbonate weathering (Kump *et al.* 1999) to expansion of reducing marine redox conditions (Hammarlund *et al.* 2012; Bartlett *et al.* 2018) or diagenetic explanations (Jones *et al.* 2020). Kozik *et al.* (2022*a*) have presented a unique perspective that integrates sea-level, new marine redox proxy data ($\delta^{34}S$, I/Ca ratios) and climate records throughout the LOME interval from three separate marine basins (see above for more details on redox proxies). These integrated records suggest that vacillating anoxic and euxinic conditions were tied to climatic cooling and glacioeustacy through intensification of thermohaline circulation and increased deep-water formation around Gondwanan margins.

The collective data over the last couple of decades suggest that a combination of cooling temperatures and the reduction of habitable space on shelves and in epeiric seaways owing to eustatic sea-level fall culminated in the traditional first LOME pulse near the Katian–Hirnantian boundary (e.g. Saupe *et al.* 2020). Consistent with this hypothesis, the first appearance of bedded chert in the Monitor Range section, suggesting an increase in local upwelling (Finney *et al.* 1999; Pope and Steffen 2003), coincides with indicators of local sea-level fall in other basins, such as the Anticosti and the Baltic basins (Desrochers *et al.* 2010; Ghienne *et al.* 2014; Kiipli and Kiipli 2020). This enhanced ocean circulation may have in turn intensified local upwelling around continental margins throughout the globe, thus leading to more local primary productivity, enhancing global carbon burial and locally pervasive anoxia (Zou *et al.* 2018; Kozik *et al.* 2022*a*, *b*). These new marine redox-linked hypotheses for the LOME (Bartlett *et al.* 2018; Dahl *et al.* 2021; Kozik *et al.* 2022*a*, *b*) provide clearer and more independent evidence for the HICE to be linked to increases in organic matter burial and associated drawdown of atmospheric CO_2. However, linking all geochemical proxy records from low-latitude settings to a glacioeustatic sea-level driver remains challenging. It seems clear that more work is needed to better understand the amplifying/dampening effects that the long-term carbon and oxygen cycles have on climate and sea-level throughout the Hirnantian.

Sea-level records for the late Hirnantian all indicate a major rise and changes in global marine redox conditions have been documented to be coincident with this eustatic sea-level rise and invoked as a causal mechanism for the traditional second LOME pulse during the late Hirnantian (Harper *et al.* 2014). As Gondwanan ice sheets melted and the late Hirnantian climate warmed (Finnegan *et al.* 2011), marine stratification and chemocline migration during eustatic sea-level rise probably played an important role in the second LOME pulse (Pohl *et al.* 2017). δ^{238}U records from carbonates on western Anticosti Island (Bartlett *et al.* 2018) – along with δ^{98}Mo and δ^{238}U data, Mo concentrations and iron speciation from organic-rich shale successions (Hammarlund *et al.* 2012; Zhou *et al.* 2015; Zou *et al.* 2018; Stockey *et al.* 2020) – indicate a return to widespread reducing conditions in global oceans during this time. Additionally, I/Ca and sulfur isotope datasets are consistent with a shift to more reducing conditions in latest Ordovician oceans (Pohl *et al.* 2021; Kozik *et al.* 2022*a*). Increased reducing conditions along continental margins during late Hirnantian time would have largely tracked eustatic sea-level rise, and the coincident warming sea-surface temperatures would have led to decreased O_2 solubility and circulation. This is consistent with the widespread black shale deposits of late Hirnantian–early Silurian age documented from multiple palaeocontinents and basins (Melchin *et al.* 2013). A recent study of thallium isotopes throughout the LOME interval suggests that oxygen-minimum zones probably expanded from deep shelf/slope to shallower areas on the continental shelf during the late Hirnantian–early Silurian and this increased the overall areal extent of seafloor overlain by anoxic and euxinic bottom waters (Kozik *et al.* 2022*b*). While it is clear that many recent investigations have highlighted the role of anoxia in the LOME, more work is needed to resolve discrepancies between palaeooceaonographic models and the local to global palaeoredox proxy datasets throughout the Hirnantian (Bartlett *et al.* 2018; Pohl *et al.* 2021; Kozik *et al.* 2022*a*, *b*).

In summary, geochemical datasets and modelling suggest widespread ventilation of marine environments followed by enhanced weathering of exposed carbonate platforms during the late Katian–early Hirnantian. This sequence of events could have resulted from the growth of Gondwanan ice sheets, enhanced thermohaline circulation that cooled SSTs and potentially increased deeper ocean oxygenation, therefore reducing sulfidic conditions in the global oceans (Kozik *et al.* 2022*a*). However, non-sulfidic anoxic conditions remained pervasive throughout shallow shelf settings owing to attendant increases in productivity resulting from increased upwelling and ocean circulation (Kozik *et al.* 2022*a*, *b*). These relationships indicate that a unique combination of reducing marine conditions, climatic cooling and glacioeustacy led to the first LOME pulse. Subsequently, deglacial eustacy during the late Hirnantian may have coincided with warming temperatures and deoxygenation, and decreased ocean circulation led to an expansion of global euxinic conditions, broadly coincident with the second LOME pulse. However, local sea-level records are predicted to have strongly deviated from the global eustacy curves generated during this time (Creveling *et al.* 2018; Pohl and Austermann 2018). Future work on the Hirnantian should focus on carefully constrained and more detailed integration of eustatic sea-level and geochemical records of climate and environmental change with palaeontological records of mass extinction, survival and recovery. Additionally, future work should also include integration of proxy records of silicate weathering with sensitivities on glacial–interglacial timescales (e.g. osmium and lithium isotopes; Finlay *et al.* 2010; Pogge von Strandmann *et al.* 2017), and geochemical proxies for changes in marine primary productivity (e.g. P, Ba, Ni, Cu; Tribovillard *et al.* 2006).

Future directions

The Ordovician Earth system and climate fluctuations have been the subject of a vigorous and productive body of work over the past two decades, but many questions still remain and new questions have arisen. This collective effort by the global community has provided new insights on major events such as the timing and potential causes of the GOBE (Servais *et al.* 2008; Trotter *et al.* 2008; Rasmussen *et al.* 2016; Edwards *et al.* 2017; Stigall *et al.* 2019), cooling and (de)oxygenation during the Hirnantian Glaciation (Finnegan *et al.* 2012; Jones and Fike 2013; Young *et al.* 2020; Kozik *et al.* 2022*a*, *b*) and changes in weathering and the transition from a greenhouse to icehouse state (Young *et al.* 2009; Conwell *et al.* 2022). Still, questions and major tasks remain and should be the focus of research for the next few decades, some of which include:

(1) The Dapingian–Darriwilian stages appear to span a critical time interval marked by the changes in continental weathering rates with possible cooling, oxygenation of the atmosphere and continued marine biodiversification. This entails questions, such as: what is the precise timing of these events, how are they possibly interrelated and were any of them causal to the others?

(2) Palaeotemperature estimates have come a long way, where δ^{18}O isotopes measured from brachiopod calcite and conodont apatite suggest a long-term cooling event, but the questions that remain are: what was the cause of this cooling and can clumped isotopes of well-preserved biominerals (i.e. conodont apatite) be used

to resolve the timing and magnitude of temperature variations? Are second-order trends within palaeotemperature proxies reproducible and what processes are they reflective of? How can spatiotemporal differences between records be explained?

(3) Recent modelling studies are apparently in conflict with each other where some models suggest that modern atmospheric O_2 levels were reached by the Mid-Late Ordovician (Edwards *et al.* 2017), whereas other studies suggest modern O_2 levels were not reached until the Devonian (Krause *et al.* 2018; Lenton *et al.* 2018). Thus, it is clear that more detailed proxy-based palaeoredox studies are needed to continue to refine and test these large discrepancies within ocean–atmosphere oxygen models. How dynamic was the Ordovician marine–atmosphere redox landscape? When and at what approximate stratigraphic levels/times did (de)oxygenation occur throughout the Ordovician? How can we reconcile these oxygen modelling differences?

(4) Studies of weathering have focused on Sr and Nd isotopes, for which convincing evidence exists for mafic (basaltic) weathering occurring during the middle Darriwilian to Sandbian interval of the Taconic Orogeny. Can we recognize this major change in Ordovician silicate weathering in other proxies that respond on shorter timescales than Sr isotopes (i.e. lithium and osmium isotopes)? Did silicate weathering play an important role in modulating climate during intervals within the Middle to Late Ordovician where glacioeustacy has been invoked?

Acknowledgements We thank Alexandre Pohl, Bertrand Lefebvre and Elise Nardin for their detailed and constructive comments that significantly improved this review chapter. We also thank Thomas Servais for editorial direction.

Competing interests The authors declare that they have no known competing financial interests or personal relationships that could have appeared to influence the work reported in this paper.

Author contributions **SAY**: Conceptualization (lead), Supervision (lead), writing – original draft (lead), Writing – review & editing (lead); **CTE**: writing – original draft (equal), Writing – review & editing (equal); **LA**: writing – original draft (Supporting), Writing – review & editing (Supporting); **AL**: writing – original draft (Supporting), Writing – review & editing (Supporting); **MRS**: writing – original draft (Supporting), Writing – review & editing (Supporting).

Funding This research received no specific grant from any funding agency in the public, commercial, or not-for-profit sectors.

Data availability Data sharing is not applicable to this article as no new datasets were generated, presented or analysed during the current study. All data presented are previously published and available through data repositories found within the respective references cited within Figure 1.

References

Abanda, P.A. and Hannigan, R.E. 2006. Effect of diagenesis on trace element partitioning in shales. *Chemical Geology*, **230**, 42–59, https://doi.org/10.1016/j.chemgeo.2005.11.011

Ainsaar, L., Meidla, T. and Martma, T. 1999. Evidence for a widespread carbon isotopic event associated with late Middle Ordovician sedimentological and faunal changes in Estonia. *Geological Magazine*, **136**, 49–62, https://doi.org/10.1017/S001675689900223X

Ainsaar, L., Meidla, T. and Martma, T. 2004. The Middle Caradoc facies and faunal turnover in the Late Ordovician Baltoscandian palaeobasin. *Palaeogeography, Palaeoclimatology, Palaeoecology*, **210**, 119–133, https://doi.org/10.1016/j.palaeo.2004.02.046

Ainsaar, L., Kaljo, D., Martma, T., Meidla, T., Männik, P., Nõlvak, J. and Tinn, O. 2010. Middle and Upper Ordovician carbon isotope chemostratigraphy in Baltoscandia: a correlation standard and clues to environmental history. *Palaeogeography, Palaeoclimatology, Palaeoecology*, **294**, 189–201, https://doi.org/10.1016/j.palaeo.2010.01.003

Ainsaar, L., Männik, P., Dronov, A.V., Izokh, O.P., Meidla, T. and Tinn, O. 2015. Carbon isotope chemostratigraphy and conodonts of the Middle–Upper Ordovician succession in the Tungus Basin, *Siberian Craton. Palaeoworld*, **24**, 123–135, https://doi.org/10.1016/j.palwor.2015.03.002

Albanesi, G.L., Barnes, C.R., Trotter, J.A., Williams, I.S. and Bergström, S.M. 2020. Comparative Lower–Middle Ordovician conodont oxygen isotope palaeothermometry of the Argentine Precordillera and Laurentian margins. *Palaeogeography, Palaeoclimatology, Palaeoecology*, **549**, 109115, https://doi.org/10.1016/j.palaeo.2019.03.016

Algeo, T.J. and Lyons, T.W. 2006. Mo-total organic carbon covariation in modern anoxic marine environments: Implications for analysis of paleoredox and paleohydrographic conditions. *Paleoceanography*, **21**, Pa1016, https://doi.org/10.1029/2004pa001112

Avila, T.D., Saltzman, M.R., Adiatma, Y.D., Griffith, E.M., Joachimski, M.M. and Olesik, J.W. 2022. Role of seafloor production versus continental basalt weathering in Middle to Late Ordovician seawater $^{87}Sr/^{86}Sr$ and climate. *Earth and Planetary Science Letters*, **593**, 117641, https://doi.org/10.1016/j.epsl.2022.117641

Azmy, K., Veizer, J., Bassett, M.G. and Copper, P. 1998. Oxygen and carbon isotopic composition of Silurian brachiopods: Implications for coeval seawater and glaciations. *Geological Society of America Bulletin*, **110**, 1499–1512, https://doi.org/10.1130/0016-7606(1998)110<1499:Oacico>2.3.Co;2

Barney, B.B. and Grossman, E.L. 2022. Reassessment of ocean paleotemperatures during the Late Ordovician. *Geology*, https://doi.org/10.1130/G49422.1

Bartlett, R., Elrick, M., Wheeley, J.R., Polyak, V., Desrochers, A. and Asmerom, Y. 2018. Abrupt global-ocean anoxia during the Late Ordovician–early Silurian detected using uranium isotopes of marine carbonates. *Proceedings of the National Academy of Sciences of the United States of America*, **115**, 5896–5901, https://doi.org/10.1073/pnas.1802438115

Bergmann, K.D., Finnegan, S., Creel, R., Eiler, J.M., Hughes, N.C., Popov, L.E. and Fischer, W.W. 2018. A paired apatite and calcite clumped isotope thermometry approach to estimating Cambro-Ordovician seawater temperatures and isotopic composition. *Geochimica et Cosmochimica Acta*, **224**, 18–41, https://doi.org/10.1016/j.gca.2017.11.015

Bergström, S.M., Chen, X., Gutierrez-Marco, J.C. and Dronov, A. 2009*a*. The new chronostratigraphic classification of the Ordovician System and its relations to major regional series and stages and to $\delta^{13}C$ chemostratigraphy. *Lethaia*, **42**, 97–107, https://doi.org/10.1111/j.1502-3931.2008.00136.x

Bergström, S.M., Xu, C., Schmitz, B., Young, S., Jia-Yu, R. and Saltzman, M.R. 2009*b*. First documentation of the Ordovician Guttenberg $\delta^{13}C$ excursion (GICE) in Asia: chemostratigraphy of the Pagoda and Yanwashan formations in southeastern China. *Geological Magazine*, **146**, 1–11, https://doi.org/10.1017/S0016756808005748

Bergström, S.M., Schmitz, B., Saltzman, M.R. and Huff, W.D. 2010*a*. The Upper Ordovician Guttenberg $\delta^{13}C$ excursion (GICE) in North America and Baltoscandia: occurrence, chronostratigraphic significance, and paleoenvironmental relationships. *Geological Society of America Special Papers*, **466**, 37–67, https://doi.org/10.1130/2010.2466(04)

Bergström, S.M., Young, S. and Schmitz, B. 2010*b*. Katian (Upper Ordovician) $\delta^{13}C$ chemostratigraphy and sequence stratigraphy in the United States and Baltoscandia: a regional comparison. *Palaeogeography, Palaeoclimatology, Palaeoecology*, **296**, 217–234, https://doi.org/10.1016/j.palaeo.2010.02.035

Bergström, S.M., Saltzman, M.R., Leslie, S.A., Ferretti, A. and Young, S.A. 2015. Trans-Atlantic application of the Baltic Middle and Upper Ordovician carbon isotope zonation. *Estonian Journal of Earth Sciences*, **64**, 8–12, https://doi.org/10.3176/earth.2015.02

Bergström, S.M., Kleffner, M. and Eriksson, M.E. 2020. Upper Katian (Upper Ordovician) trans-Atlantic $\delta^{13}C$ chemostratigraphy: the geochronological equivalence of the ELKHORN and PAROVEJA excursions and its implications. *Lethaia*, **53**, 199–216, https://doi.org/10.1111/let.12351

Berner, R.A. 1990. Atmospheric carbon-dioxide levels over Phanerozoic time. *Science*, **249**, 1382–1386, https://doi.org/10.1126/science.249.4975.1382

Berner, R.A. 2001. Modeling atmospheric O_2 over Phanerozoic time. *Geochimica et Cosmochimica Acta*, **65**, 685–694, https://doi.org/10.1016/S0016-7037(00)00572-X

Berner, R.A. 2006. GEOCARBSULF: a combined model for Phanerozoic atmospheric O_2 and CO_2. *Geochimica et Cosmochimica Acta*, **70**, 5653–5664, https://doi.org/10.1016/j.gca.2005.11.032

Bond, D.P.G. and Grasby, S.E. 2020. Late Ordovician mass extinction caused by volcanism, warming, and anoxia, not cooling and glaciation. *Geology*, **48**, 777–781, https://doi.org/10.1130/G47377.1

Brand, U., Davis, A.M., Shaver, K.K., Blamey, N.J.F., Heizler, M. and Lecuyer, C. 2021. Atmospheric oxygen of the Paleozoic. *Earth-Science Reviews*, **216**, 103560, https://doi.org/10.1016/j.earscirev.2021.103560

Brenchley, P.J., Marshall, J.D. *et al*. 1994. Bathymetric and isotopic evidence for a short-lived Late Ordovician glaciation in a greenhouse period. *Geology*, **22**, 295–298, https://doi.org/10.1130/0091-7613(1994)022<0295:BAIEFA>2.3.CO;2

Brenchley, P.J., Carden, G.A. *et al*. 2003. High-resolution stable isotope stratigraphy of Upper Ordovician sequences: constraints on the timing of bioevents and environmental changes associated with mass extinction and glaciation. *Geological Society of America Bulletin*, **115**, 89–104, https://doi.org/10.1130/0016-7606(2003)115<0089:Hrsiso>2.0.Co;2

Buggisch, W., Joachimski, M.M., Lehnert, O., Bergström, S.M., Repetski, J.E. and Webers, G.F. 2010. Did intense volcanism trigger the first Late Ordovician icehouse? *Geology*, **38**, 327–330, https://doi.org/10.1130/G30577.1

Came, R.E., Eiler, J.M., Veizer, J., Azmy, K., Brand, U. and Weidman, C.R. 2007. Coupling of surface temperatures and atmospheric CO_2 concentrations during the Palaeozoic era. *Nature*, **449**, 198–201, https://doi.org/10.1038/nature06085

Cherns, L. and Wheeley, J.R. 2007. A pre-Himantian (Late Ordovician) interval of global cooling – the Boda event re-assessed. *Palaeogeography, Palaeoclimatology, Palaeoecology*, **251**, 449–460, https://doi.org/10.1016/j.palaeo.2007.04.010

Cocks, L.R.M. and Torsvik, T.H. 2021. Ordovician palaeogeography and climate change. *Gondwana Research*, **100**, 53–72, https://doi.org/10.1016/j.gr.2020.09.008

Conwell, C.T., Saltzman, M.R., Edwards, C.T., Griffith, E.M. and Adiatma, Y.D. 2022. Nd isotopic evidence for enhanced mafic weathering leading to Ordovician cooling. *Geology*, **50**, 886–890, https://doi.org/10.1130/G49860.1

Cramer, B.D. and Jarvis, I. 2020. Carbon isotope stratigraphy. In: Gradstein, F.M., Ogg, J.G., Schmitz, M.D. and Ogg, G.M. (eds) *Geologic Time Scale 2020*. Elsevier, 309–343.

Creveling, J.R., Finnegan, S., Mitrovica, J.X. and Bergmann, K.D. 2018. Spatial variation in Late Ordovician glacioeustatic sea-level change. *Earth and Planetary Science Letters*, **496**, 1–9, https://doi.org/10.1016/j.epsl.2018.05.008

Crowley, T.J. and Baum, S.K. 1995. Reconciling Late Ordovician (440-Ma) glaciation with very high (14×) CO_2 levels. *Journal of Geophysical Research-Atmospheres*, **100**, 1093–1101, https://doi.org/10.1029/94jd02521

Dabard, M.P., Loi, A., Paris, F., Ghienne, J.F., Pistis, M. and Vidal, M. 2015. Sea-level curve for the Middle to early Late Ordovician in the Armorican Massif (western

France): icehouse third-order glacio-eustatic cycles. *Palaeogeography, Palaeoclimatology, Palaeoecology*, **436**, 96–111, https://doi.org/10.1016/j.palaeo.2015.06.038

Dahl, T.W., Hammarlund, E.U. *et al*. 2010. Devonian rise in atmospheric oxygen correlated to the radiations of terrestrial plants and large predatory fish. *Proceedings of the National Academy of Sciences of the United States of America*, **107**, 17911–17915, https://doi.org/10.1073/pnas.1011287107/-/DCSupplemental

Dahl, T.W., Hammarlund, E.U., Rasmussen, C.M., Bond, D.P.G. and Canfield, D.E. 2021. Sulfidic anoxia in the oceans during the Late Ordovician mass extinctions-insights from molybdenum and uranium isotopic global redox proxies. *Earth-Science Reviews*, **220**, 103748, https://doi.org/10.1016/j.earscirev.2021.103748

Desrochers, A., Farley, C., Achab, A., Asselin, E. and Riva, J.F. 2010. A far-field record of the end Ordovician glaciation: the Ellis Bay Formation, Anticosti Island, Eastern Canada. *Palaeogeography Palaeoclimatology Palaeoecology*, **296**, 248–263, https://doi.org/10.1016/j.palaeo.2010.02.017

Edward, O., Korte, C. *et al*. 2022. A Baltic perspective on the Early to Early Late Ordovician $\delta^{13}C$ and $\delta^{18}O$ records and its paleoenvironmental significance. *Paleoceanography and Paleoclimatology*, **37**, https://doi.org/10.1029/2021PA004309

Edwards, C.T. 2019. Links between early Paleozoic oxygenation and the Great Ordovician Biodiversification Event (GOBE): a review. *Palaeoworld*, **28**, https://doi.org/10.1016/j.palwor.2018.08.006

Edwards, C.T., Saltzman, M.R., Royer, D.L. and Fike, D.A. 2017. Oxygenation as a driver of the Great Ordovician Biodiversification Event. *Nature Geoscience*, **10**, 925–929, https://doi.org/10.1038/s41561-017-0006-3

Edwards, C.T., Fike, D.A. and Saltzman, M.R. 2019. Testing carbonate-associated sulfate (CAS) extraction methods for sulfur isotope stratigraphy: A case study of a Lower-Middle Ordovician carbonate succession, Shingle Pass, Nevada, USA. *Chemical Geology*, **529**, https://doi.org/ARTN 119297 10.1016/j.chemgeo.2019.119297

Edwards, C.T., Fike, D.A., Saltzman, M.R., Lu, W.Y. and Lu, Z.L. 2018. Evidence for local and global redox conditions at an Early Ordovician (Tremadocian) mass extinction. *Earth and Planetary Science Letters*, **481**, 125–135, https://doi.org/10.1016/j.epsl.2017.10.002

Edwards, C.T., Jones, C.M., Quinton, P.C. and Fike, D.A. 2022. Oxygen isotope (delta(^{18}O)) trends measured from Ordovician conodont apatite using secondary ion mass spectrometry (SIMS): implications for paleothermometry studies. *Geological Society of America Bulletin*, **134**, 261–274, https://doi.org/10.1130/B35891.1

Elrick, M., Reardon, D., Labor, W., Martin, J., Desrochers, A. and Pope, M. 2013. Orbital-scale climate change and glacioeustasy during the early Late Ordovician (pre-Hirnantian) determined from $\delta^{18}O$ values in marine apatite. *Geology*, **41**, 775–778, https://doi.org/10.1130/G34363.1

Finlay, A.J., Selby, D. and Grocke, D.R. 2010. Tracking the Hirnantian glaciation using Os isotopes. *Earth and Planetary Science Letters*, **293**, 339–348, https://doi.org/10.1016/j.epsl.2010.02.049

Finnegan, S., Bergmann, K. *et al*. 2011. The magnitude and duration of Late Ordovician–Early Silurian glaciation. *Science*, **331**, 903–906, https://doi.org/10.1126/science.1200803

Finnegan, S., Heim, N.A., Peters, S.E. and Fischer, W.W. 2012. Climate change and the selective signature of the Late Ordovician mass extinction. *Proceedings of the National Academy of Sciences of the United States of America*, **109**, 6829–6834, https://doi.org/10.1073/pnas.1117039109

Finney, S.C., Berry, W.B.N. *et al*. 1999. Late Ordovician mass extinction: a new perspective from stratigraphic sections in central Nevada. *Geology*, **27**, 215–218, https://doi.org/10.1130/0091-7613(1999)027<0215:Lomean>2.3.Co;2

Fortey, R.A. and Cocks, LRM. 2005. Late Ordovician global warming – the Boda event. *Geology*, **33**, 405–408, https://doi.org/10.1130/G21180.1

Froelich, P.N., Klinkhammer, G.P. *et al*. 1979. Early oxidation of organic-matter in pelagic sediments of the Eastern Equatorial Atlantic–Suboxic diagenesis. *Geochimica Et Cosmochimica Acta*, **43**, 1075–1090, https://doi.org/10.1016/0016-7037(79)90095-4

Geyman, E.C. and Maloof, A.C. 2019. A diurnal carbon engine explains ^{13}C-enriched carbonates without increasing the global production of oxygen. *Proceedings of the National Academy of Sciences of the United States of America*, **116**, 24433–24439, https://doi.org/10.1073/pnas.1908783116

Ghienne, J.-F., Boumendjel, K., Paris, F., Videt, B., Racheboeuf, P. and Ait Salem, H. 2007. The Cambrian–Ordovician succession in the Ougarta Range (western Algeria, North Africa) and interference of the Late Ordovician glaciation on the development of the Lower Palaeozoic transgression on northern Gondwana. *Bull. Geosci*, **82**, 183–214, https://doi.org/10.3140/bull.geosci.2007.03.183

Ghienne, J.F., Desrochers, A. *et al*. 2014. A Cenozoic-style scenario for the end-Ordovician glaciation. *Nature Communications*, **5**, 4485, https://doi.org/10.1038/ncomms5485

Gill, B.C., Lyons, T.W. and Saltzman, M.R. 2007. Parallel, high-resolution carbon and sulfur isotope records of the evolving Paleozoic marine sulfur reservoir. *Palaeogeography Palaeoclimatology Palaeoecology*, **256**, 156–173, https://doi.org/10.1016/J.Palaeo.2007 .02.030

Gill, B.C., Lyons, T.W., Young, S.A., Kump, L.R., Knoll, A.H. and Saltzman, M.R. 2011. Geochemical evidence for widespread euxinia in the Later Cambrian ocean. *Nature*, **469**, 80–83, https://doi.org/10.1038/Nature09700

Goldberg, S.L., Present, T.M., Finnegan, S. and Bergmann, K.D. 2021. A high-resolution record of early Paleozoic climate. *Proceedings of the National Academy of Sciences*, **118**, e2013083118, https://doi.org/10.1073/pnas.2013083118

Goldman, D., Sadler, P.M., Leslie, S.A., Melchin, M.J., Agterberg, F.P. and Gradstein, F.M. 2020. The Ordovician Period. In: Gradstein, F.M., Ogg, J.G., Schmitz, M.D. and Ogg, G.M. (eds) *Geologic Time Scale 2020*. Elsevier, 631–694.

Gorjan, P., Kaiho, K., Fike, D.A. and Xu, C. 2012. Carbon- and sulfur-isotope geochemistry of the Hirnantian (Late

Ordovician) Wangjiawan (Riverside) section, South China: global correlation and environmental event interpretation. *Palaeogeography, Palaeoclimatology, Palaeoecology*, **337–338**, 14–22, https://doi.org/10.1016/j.palaeo.2012.03.021

Grossman, E.L. and Joachimski, M.M. 2022. Ocean temperatures through the Phanerozoic reassessed. *Scientific Reports*, **12**, 8938, https://doi.org/10.1038/s41598-022-11493-1

Hammarlund, E.U., Dahl, T.W. *et al*. 2012. A sulfidic driver for the end-Ordovician mass extinction. *Earth and Planetary Science Letters*, **331**, 128–139, https://doi.org/10.1016/J.Epsl.2012.02.024

Haq, B.U. and Schutter, S.R. 2008. A chronology of Paleozoic sea-level changes. *Science*, **322**, 64–68, https://doi.org/10.1126/science.1161648

Harper, D.A.T., Hammarlund, E.U. and Rasmussen, C.M.O. 2014. End Ordovician extinctions: a coincidence of causes. *Gondwana Research*, **25**, 1294–1307, https://doi.org/10.1016/j.gr.2012.12.021

Hennessy, J.F. and Mossman, D.J. 1996. Geochemistry of Ordovician black shales at Meductic, southern Miramichi Highlands, New Brunswick. *Atlantic Geology*, **32**, 233–245, https://doi.org/10.4138/2089

Herrmann, A.D., Patzkowsky, M.E. and Pollard, D. 2003. Obliquity forcing with 8–12 times preindustrial levels of atmospheric pCO2 during the Late Ordovician glaciation. *Geology*, **31**, 485–488, https://doi.org/10.1130/0091-7613(2003)031<0485:Ofwtpl>2.0.Co;2

Herrmann, A.D., Haupt, B.J., Patzkowsky, M.E., Seidov, D. and Slingerland, R.L. 2004. Response of Late Ordovician paleoceanography to changes in sea level, continental drift, and atmospheric $p\mathrm{CO_2}$: potential causes for long-term cooling and glaciation. *Palaeogeography Palaeoclimatology Palaeoecology*, **210**, 385–401, https://doi.org/10.1016/j.palaeo.2004.02.034

Herrmann, A.D., Macleod, K.G. and Leslie, S.A. 2010. Did a Volcanic Mega-Eruption Cause Global Cooling during the Late Ordovician? *Palaios*, **25**, 831–836, https://doi.org/10.2110/palo.2010.p10-069r

Holmden, C., Creaser, R.A., Muehlenbachs, K., Leslie, S.A. and Bergström, S.M. 1998. Isotopic evidence for geochemical decoupling between ancient epeiric seas and bordering oceans: implications for secular curves. *Geology*, **26**, 567–570, https://doi.org/10.1130/0091-7613(1998)026<0567:IEFGDB>2.3.CO;2

Jablonski, D. 1991. Extinctions – a paleontological perspective. *Science*, **253**, 754–757, https://doi.org/10.1126/science.253.5021.754

Jaffrés, J.B.D., Shields, G.A. and Wallmann, K. 2007. The oxygen isotope evolution of seawater: A critical review of a long-standing controversy and an improved geological water cycle model for the past 3.4 billion years. *Earth-Science Reviews*, **83**, 83–122, https://doi.org/10.1016/j.earscirev.2007.04.002

Jin, J., Zhan, R. and Wu, R. 2018. Equatorial cold-water tongue in the Late Ordovician. *Geology*, **46**, 759–762, https://doi.org/10.1130/G45302.1

Jones, D.S. and Fike, D.A. 2013. Dynamic sulfur and carbon cycling through the end-Ordovician extinction revealed by paired sulfate-pyrite delta S-34. *Earth and Planetary Science Letters*, **363**, 144–155, https://doi.org/10.1016/J.Epsl.2012.12.015

Jones, D.S., Creel, R.C. and Rios, B.A. 2016. Carbon isotope stratigraphy and correlation of depositional sequences in the Upper Ordovician Ely Springs Dolostone, eastern Great Basin, USA. *Palaeogeography Palaeoclimatology Palaeoecology*, **458**, 85–101, https://doi.org/10.1016/j.palaeo.2016.01.036

Jones, D.S., Martini, A.M., Fike, D.A. and Kaiho, K. 2017. A volcanic trigger for the Late Ordovician mass extinction? Mercury data from south China and Laurentia. *Geology*, **45**, 631–634, https://doi.org/10.1130/G38940.1

Jones, D.S., Brothers, R.W., Ahm, A.S.C., Slater, N., Higgins, J.A. and Fike, D.A. 2020. Sea level, carbonate mineralogy, and early diagenesis controlled δ^{13}C records in Upper Ordovician carbonates. *Geology*, **48**, 194–199, https://doi.org/10.1130/G46861.1

Jones, L.A. and Eichenseer, K. 2022. Uneven spatial sampling distorts reconstructions of Phanerozoic seawater temperature. *Geology*, **50**, 238–242, https://doi.org/10.1130/G49132.1

Kiipli, E. and Kiipli, T. 2020. Hirnantian sea-level changes in the Baltoscandian Basin, a review. *Palaeogeography Palaeoclimatology Palaeoecology*, **540**, 109524, https://doi.org/10.1016/j.palaeo.2019.109524

Kim, S.-T. and O'Neil, J.R. 1997. Equilibrium and nonequilibrium oxygen isotope effects in synthetic carbonates. *Geochimica et Cosmochimica Acta*, **61**, 3461–3475, https://doi.org/10.1016/S0016-7037(97)00169-5

Kolodny, Y., Luz, B. and Navon, O. 1983. Oxygen isotope variations in phosphate of biogenic apatites, I. Fish bone apatite rechecking the rules of the game. *Earth and Planetary Science Letters*, **64**, 61, https://doi.org/10.1016/0012-821X(83)90100-0

Kozik, N.P., Gill, B.C., Owens, J.D., Lyons, T.W. and Young, S.A. 2022*a*. Geochemical records reveal protracted and differential marine redox change associated with Late Ordovician climate and mass extinctions. *Agu Advances*, **3**, https://doi.org/10.1029/2021AV000563

Kozik, N.P., Young, S.A. *et al*. 2022*b*. Rapid marine oxygen variability: driver of the Late Ordovician mass extinction. *Sci Adv*, **8**, eabn8345, https://doi.org/10.1126/sciadv.abn8345

Krause, A.J., Mills, B.J.W., Zhang, S., Planavsky, N.J., Lenton, T.M. and Poulton, S.W. 2018. Stepwise oxygenation of the Paleozoic atmosphere. *Nature Communications*, **9**, https://doi.org/ARTN 4081.10.1038/s41467-018-06383-y

Kump, L.R., Arthur, M.A., Patzkowsky, M.E., Gibbs, M.T., Pinkus, D.S. and Sheehan, P.M. 1999. A weathering hypothesis for glaciation at high atmospheric $p\mathrm{CO_2}$ during the Late Ordovician. *Palaeogeography Palaeoclimatology Palaeoecology*, **152**, 173–187, https://doi.org/10.1016/S0031-0182(99)00046-2

Kumpulainen, R.A. 2007. The Ordovician glaciation in Eritrea and Ethiopia, NE Africa. *Glacial Sedimentary Processes and Products*, 321–342, https://doi.org/10.1002/9781444304435.ch18

LaPorte, D.F., Holmden, C. *et al*. 2009. Local and global perspectives on carbon and nitrogen cycling during the Hirnantian glaciation. *Palaeogeography Palaeoclimatology Palaeoecology*, **276**, 182–195, https://doi.org/10.1016/j.palaeo.2009.03.009

Lécuyer, C., Amiot, R., Touzeau, A. and Trotter, J. 2013. Calibration of the phosphate δ^{18}O thermometer with carbonate–water oxygen isotope fractionation equations. *Chemical Geology*, **347**, 217–226, https://doi.org/10.1016/j.chemgeo.2013.03.008

Lenton, T.M., Dahl, T.W., Daines, S.J., Mills, B.J.W., Ozaki, K., Saltzman, M.R. and Porada, P. 2016. Earliest land plants created modern levels of atmospheric oxygen. *Proceedings of the National Academy of Sciences of the United States of America*, **113**, 9704–9709, https://doi.org/10.1073/pnas.1604787113

Lenton, T.M., Daines, S.J. and Mills, B.J.W. 2018. COPSE reloaded: an improved model of biogeochemical cycling over Phanerozoic time. *Earth-Science Reviews*, **178**, 1–28, https://doi.org/10.1016/j.earscirev.2017.12.004

Lindskog, A. and Eriksson, M.E. 2017. Megascopic processes reflected in the microscopic realm: sedimentary and biotic dynamics of the Middle Ordovician 'orthoceratite limestone' at Kinnekulle, Sweden. *Gff*, **139**, 163–183, https://doi.org/10.1080/11035897.2017.1291538

Lindskog, A. and Young, S.A. 2019. Dating of sedimentary rock intervals using visual comparison of carbon isotope records: a comment on the recent paper by Bergstrom *et al.* concerning the age of the Winneshiek Shale. *Lethaia*, **52**, 299–303, https://doi.org/10.1111/let.12316

Lindskog, A., Eriksson, M.E., Bergstrom, S.M. and Young, S.A. 2019. Lower-Middle Ordovician carbon and oxygen isotope chemostratigraphy at Hallekis, Sweden: implications for regional to global correlation and palaeoenvironmental development. *Lethaia*, **52**, 204–219, https://doi.org/10.1111/let.12307

Lindström, M. 1979. Diagenesis of lower Ordovician hardgrounds in Sweden. *Geologica et Palaeontologica*, **13**, 9–30.

Liu, C.G., Li, G.R., Wang, D.W., Liu, Y.L., Luo, M.X. and Shao, X.M. 2016. Middle Upper Ordovician (Darriwilian–Early Katian) positive carbon isotope excursions in the northern Tarim Basin, northwest China: Implications for stratigraphic correlation and paleoclimate. *Journal of Earth Science*, **27**, 317–328, https://doi.org/10.1007/s12583-016-0696-2

Liu, K., Jiang, M., Zhang, L. and Chen, D. 2022. A new high-resolution palaeotemperature record during the Middle–Late Ordovician transition derived from conodont δ^{18}O palaeothermometry. *Journal of the Geological Society*, **179**, jgs2021-148, https://doi.org/10.1144/jgs2021-148

Loi, A., Ghienne, J.F. *et al*. 2010. The Late Ordovician glacio-eustatic record from a high-latitude storm-dominated shelf succession: the Bou Ingarf section (Anti-Atlas, Southern Morocco). *Palaeogeography, Palaeoclimatology, Palaeoecology*, **296**, 332–358, https://doi.org/10.1016/j.palaeo.2010.01.018

Longinelli, A. and Nuti, S. 1973. Revised phosphate–water isotopic temperature scale. *Earth and Planetary Science Letters*, **19**, 373–376, https://doi.org/10.1016/0012-821X(73)90088-5

Lyons, T.W., Reinhard, C.T. and Scott, C. 2009. Redox redux. *Geobiology*, **7**, 489–494, https://doi.org/10.1111/j.1472-4669.2009.00222.x

Macdonald, F.A., Swanson-Hysell, N.L., Park, Y., Lisiecki, L. and Jagoutz, O. 2019. Arc-continent collisions in the tropics set Earth's climate state. *Science*, **364**, 181–184, https://doi.org/10.1126/science.aav5300

Männik, P., Lehnert, O., Nõlvak, J. and Joachimski, M.M. 2021. Climate changes in the pre-Hirnantian Late Ordovician based on $\delta^{18}O_{phos}$ studies from Estonia. *Palaeogeography, Palaeoclimatology, Palaeoecology*, **569**, 110347, https://doi.org/10.1016/j.palaeo.2021.110347

Marcilly, C.M., Maffre, P. *et al*. 2022. Understanding the early Paleozoic carbon cycle balance and climate change from modelling. *Earth and Planetary Science Letters*, **594**, https://doi.org/10.1016/j.epsl.2022.117717

McKenzie, N.R., Horton, B.K., Loomis, S.E., Stockli, D.F., Planavsky, N.J. and Lee, C.T.A. 2016. Continental arc volcanism as the principal driver of icehouse–greenhouse variability. *Science*, **352**, 444–447, https://doi.org/10.1126/science.aad5787

Melchin, M.J. and Holmden, C. 2006. Carbon isotope chemostratigraphy in Arctic Canada: sea-level forcing of carbonate platform weathering and implications for Hirnantian global correlation. *Palaeogeography Palaeoclimatology Palaeoecology*, **234**, 186–200, https://doi.org/10.1016/j.palaeo.2005.10.009

Melchin, M.J., Mitchell, C.E., Holmden, C. and Storch, P. 2013. Environmental changes in the Late Ordovicianearly Silurian: review and new insights from black shales and nitrogen isotopes. *Geological Society of America Bulletin*, **125**, 1635–1670, https://doi.org/10.1130/B30812.1

Munnecke, A., Zhang, Y., Liu, X. and Cheng, J. 2011. Stable carbon isotope stratigraphy in the Ordovician of South China. *Palaeogeography, Palaeoclimatology, Palaeoecology*, **307**, 17–43, https://doi.org/10.1016/j.palaeo.2011.04.015

Nardin, E., Godderis, Y., Donnadieu, Y., Le Hir, G., Blakey, R.C., Puceat, E. and Aretz, M. 2011. Modeling the early Paleozoic long-term climatic trend. *Geological Society of America Bulletin*, **123**, 1181–1192, https://doi.org/10.1130/B30364.1

Owens, J.D. 2019. Application of thallium isotopes: tracking marine oxygenation through manganese oxide burial. *Application of Thallium Isotopes: Tracking Marine Oxygenation through Manganese Oxide Burial*, 1–+, https://doi.org/10.1017/9781108688697

Panchuk, K.M., Holmden, C.E. and Leslie, S.A. 2006. Local controls on carbon cycling in the Ordovician midcontinent region of North America, with implications for carbon isotope secular curves. *Journal of Sedimentary Research*, **76**, 200–211, https://doi.org/10.2110/jsr.2006.017

Pancost, R.D., Freeman, K.H., Herrmann, A.D., Patzkowsky, M.E., Ainsaar, L. and Martma, T. 2013. Reconstructing Late Ordovician carbon cycle variations. *Geochimica Et Cosmochimica Acta*, **105**, 433–454, https://doi.org/10.1016/j.gca.2012.11.033

Pietzner, H., Vahl, J., Werner, H. and Ziegler, W. 1968. Zur chemischen zusammensetzung und mikromorphologie der conodonten. *Palaeontographica Abteilung A, Paläozoologie, Stratigraphie*, **128**, 115–152.

Pogge von Strandmann, P.A.E., Desrochers, A., Murphy, M.J., Finlay, A.J., Selby, D. and Lenton, T.M. 2017. Global climate stabilisation by chemical weathering during the Hirnantian glaciation. *Geochemical*

Perspectives Letters, **3**, 230–237, https://doi.org/10.7185/230.geochemlet.1726

Pohl, A. and Austermann, J. 2018. A sea-level fingerprint of the Late Ordovician ice-sheet collapse. *Geology*, **46**, 595–598, https://doi.org/10.1130/G40189.1

Pohl, A., Donnadieu, Y., Le Hir, G. and Ferreira, D. 2017. The climatic significance of Late Ordovician–early Silurian black shales. *Paleoceanography*, **32**, 397–423, https://doi.org/10.1002/2016pa003064

Pohl, A., Donnadieu, Y., Le Hir, G., Ladant, J.B., Dumas, C., Alvarez-Solas, J. and Vandenbroucke, T.R.A. 2016. Glacial onset predated Late Ordovician climate cooling. *Paleoceanography*, **31**, 800–821, https://doi.org/10.1002/2016pa002928

Pohl, A., Lu, Z.L. *et al*. 2021. Vertical decoupling in Late Ordovician anoxia due to reorganization of ocean circulation. *Nature Geoscience*, **14**, 868–873, https://doi.org/10.1038/s41561-021-00843-9

Pohl, A., Donnadieu, Y., Le Hir, G., Buoncristiani, J.F. and Vennin, E. 2014. Effect of the Ordovician paleogeography on the (in)stability of the climate. *Climate of the Past*, **10**, 2053–2066, https://doi.org/10.5194/cp-10-2053-2014

Pohl, A., Ridgwell, A., Stockey, R.G., Thomazo, C., Keane, A., Vennin, E. and Scotese, C.R. 2022. Continental configuration controls ocean oxygenation during the Phanerozoic. *Nature*, **608**, 523–527, https://doi.org/10.1038/s41586-022-05018-z

Pope, M.C. and Steffen, J.B. 2003. Widespread, prolonged late Middle to Late Ordovician upwelling in North America: A proxy record of glaciation? *Geology*, **31**, 63–66, https://doi.org/10.1130/0091-7613(2003)031<0063:Wplmtl>2.0.Co;2

Poussart, P.F., Weaver, A.J. and Barnes, C.R. 1999. Late Ordovician glaciation under high atmospheric CO_2: a coupled model analysis. *Paleoceanography*, **14**, 542–558, https://doi.org/10.1029/1999pa900021

Pruss, S.B., Finnegan, S., Fischer, W.W. and Knoll, A.H. 2010. Carbonates in skeleton-poor seas: new insights from Cambrian and Ordovician strata of Laurentia. *Palaios*, **25**, 73–84, https://doi.org/10.2110/palo.2009.p09-101r

Pucéat, E. *et al*. 2010. Revised phosphate–water fractionation equation reassessing paleotemperatures derived from biogenic apatite. *Earth and Planetary Science Letters*, **298**, 135–142, https://doi.org/10.1016/j.epsl.2010.07.034

Quinton, P.C. and MacLeod, K.G. 2014. Oxygen isotopes from conodont apatite of the midcontinent, US: implications for Late Ordovician climate evolution. *Palaeogeography, Palaeoclimatology, Palaeoecology*, **404**, 57–66, https://doi.org/10.1016/j.palaeo.2014.03.036

Quinton, P.C., Law, S., MacLeod, K.G., Herrmann, A.D., Haynes, J.T. and Leslie, S.A. 2018*a*. Testing the early Late Ordovician cool-water hypothesis with oxygen isotopes from conodont apatite. *Geological Magazine*, **155**, 1727–1741, https://doi.org/10.1017/S0016756817000589

Quinton, P.C., Speir, L., Miller, J., Ethington, R. and Macleod, K.G. 2018*b*. Extreme heat in the early Ordovician. *Palaios*, **33**, 353–360, https://doi.org/10.2110/palo.2018.031

Rasmussen, C.M.Ø., Ullmann, C.V., Jakobsen, K.G., Lindskog, A., Hansen, J., Hansen, T. and Harper, D.A.T. 2016. Onset of main Phanerozoic marine radiation sparked by emerging Mid Ordovician icehouse. *Scientific Reports*, **6**, 1–9, https://doi.org/10.1038/srep18884

Rasmussen, J.A., Thibault, N. and Rasmussen, C.M.Ø. 2021. Middle Ordovician astrochronology decouples asteroid breakup from glacially-induced biotic radiations. *Nature Communications*, **12**, 6430, https://doi.org/10.1038/s41467-021-26396-4

Rosenau, N.A., Herrmann, A.D. and Leslie, S.A. 2012. Conodont apatite $\delta^{18}O$ values from a platform margin setting, Oklahoma, USA: implications for initiation of Late Ordovician icehouse conditions. *Palaeogeography, Palaeoclimatology, Palaeoecology*, **315**, 172–180, https://doi.org/10.1016/j.palaeo.2011.12.003

Rothman, D.H. 2002. Atmospheric carbon dioxide levels for the last 500 million years. *Proceedings of the National Academy of Sciences of the United States of America*, **99**, 4167–4171, https://doi.org/10.1073/pnas.022055499

Saltzman, M.R. 2005. Phosphorus, nitrogen, and the redox evolution of the Paleozoic oceans. *Geology*, **33**, 573–576, https://doi.org/10.1130/G21535.1

Saltzman, M.R. and Edwards, C.T. 2017. Gradients in the carbon isotopic composition of Ordovician shallow water carbonates: A potential pitfall in estimates of ancient CO_2 and O_2. *Earth and Planetary Science Letters*, **464**, 46–54, https://doi.org/10.1016/j.epsl.2017.02.011

Saltzman, M.R. and Young, S.A. 2005. Long-lived glaciation in the Late Ordovician? Isotopic and sequence-stratigraphic evidence from western Laurentia. *Geology*, **33**, 109–112, https://doi.org/10.1130/G21219.1

Saltzman, M.R., Young, S.A., Kump, L.R., Gill, B.C., Lyons, T.W. and Runnegar, B. 2011. Pulse of atmospheric oxygen during the late Cambrian. *Proceedings of the National Academy of Sciences of the United States of America*, **108**, 3876–3881, https://doi.org/10.1073/Pnas.1011836108

Saltzman, M.R., Edwards, C.T., Leslie, S.A., Dwyer, G.S., Bauer, J.A., Repetski, J.E. and Bergström, S.M. 2014. Calibration of a conodont apatite-based Ordovician $^{87}Sr/^{86}Sr$ curve to biostratigraphy and geochronology: implications for stratigraphic resolution. *Bulletin of the Geological Society of America*, **126**, 1551–1568, https://doi.org/10.1130/B31038.1

Saltzman, M.R., Edwards, C.T., Adrain, J.M. and Westrop, S.R. 2015. Persistent oceanic anoxia and elevated extinction rates separate the Cambrian and Ordovician radiations. *Geology*, **43**, 807–810, https://doi.org/10.1130/G36814.1

Saupe, E.E., Qiao, H.J. *et al*. 2020. Extinction intensity during Ordovician and Cenozoic glaciations explained by cooling and palaeogeography. *Nature Geoscience*, **13**, 65–70, https://doi.org/10.1038/s41561-019-0504-6

Schmitz, B., Harper, D.A.T. *et al*. 2008. Asteroid breakup linked to the Great Ordovician Biodiversification Event. *Nature Geoscience*, **1**, 49–53, https://doi.org/10.1038/Ngeo.2007.37

Schovsbo, N.H. 2002. Uranium enrichment shorewards in black shales: a case study from the Scandinavian. *GFF*, **124**, 107–116, https://doi.org/10.1080/11035890201 242107

Servais, T., Lehnert, O., Li, J., Mullins, G.L., Munnecke, A., Nutzel, A. and Vecoli, M. 2008. The Ordovician biodiversification: revolution in the oceanic trophic chain. *Lethaia*, **41**, 99–109, https://doi.org/10.1111/J.1502-3931.2008.00115.X

Servais, T., Cascales-Minana, B. and Harper, D.A.T. 2021. The Great Ordovician Biodiversification Event (GOBE) is not a single event. *Paleontological Research*, **25**, 315–328, https://doi.org/10.2517/2021pr001

Sheehan, P.M. 2001. The Late Ordovician mass extinction. *Annual Review of Earth and Planetary Sciences*, **29**, 331–364, https://doi.org/10.1146/annurev.earth.29.1.331

Shemesh, A., Kolodny, Y. and Luz, B. 1983. Oxygen isotope variations in phosphate of biogenic apatites, II. Phosphorite rocks. *Earth and Planetary Science Letters*, **64**, 405–416, https://doi.org/10.1016/0012-821X(83)90101-2

Shields, G.A., Carden, G.A.F., Veizer, J., Meidla, T., Rong, J.Y. and Li, R.Y. 2003. Sr, C, and O isotope geochemistry of Ordovician brachiopods: A major isotopic event around the Middle–Late Ordovician transition. *Geochimica Et Cosmochimica Acta*, **67**, 2005–2025, https://doi.org/10.1016/S0016-7037(02)01116-X

Sial, A.N., Peralta, S. *et al*. 2013. High-resolution stable isotope stratigraphy of the upper Cambrian and Ordovician in the Argentine Precordillera: Carbon isotope excursions and correlations. *Gondwana Research*, **24**, 330–348, https://doi.org/10.1016/j.gr.2012.10.014

Song, H.J., Wignall, P.B., Song, H.Y., Dai, X. and Chu, D.L. 2019. Seawater temperature and dissolved oxygen over the past 500 million years. *Journal of Earth Science*, **30**, 236–243, https://doi.org/10.1007/s12583-018-1002-2

Stigall, A.L., Edwards, C.T., Freeman, R.L. and Rasmussen, C.M.Ø. 2019. Coordinated biotic and abiotic change during the Great Ordovician Biodiversification Event: Darriwilian assembly of early Paleozoic building blocks. *Palaeogeography, Palaeoclimatology, Palaeoecology*, **530**, https://doi.org/10.1016/j.palaeo.2019.05.034

Stockey, R.G., Cole, D.B., Planavsky, N.J., Loydell, D.K., Fryda, J. and Sperling, E.A. 2020. Persistent global marine euxinia in the early Silurian. *Nature Communications*, **11**, https://doi.org/10.1038/s41467-020-15400-y

Stockey, R.G., Pohl, A., Ridgwell, A., Finnegan, S. and Sperling, E.A. 2021. Decreasing Phanerozoic extinction intensity as a consequence of Earth surface oxygenation and metazoan ecophysiology. *Proceedings of the National Academy of Sciences of the United States of America*, **118**, https://doi.org/10.1073/pnas.2101900118

Swanson-Hysell, N.L. and Macdonald, F.A. 2017. Tropical weathering of the Taconic orogeny as a driver for Ordovician cooling. *Geology*, **45**, 719–722, https://doi.org/10.1130/G38985.1

Thompson, C.K. and Kah, L.C. 2012. Sulfur isotope evidence for widespread euxinia and a fluctuating oxycline in Early to Middle Ordovician greenhouse oceans. *Palaeogeography Palaeoclimatology Palaeoecology*, **313**, 189–214, https://doi.org/10.1016/J.Palaeo.2011.10.020

Tostevin, R. and Mills, B.J.W. 2020. Reconciling proxy records and models of Earth's oxygenation during the Neoproterozoic and Palaeozoic. *Interface Focus*, **10**, https://doi.org/ARTN 20190137 10.1098/rsfs.2019.0137

Trela, W., Krzemińska, E., Jewuła, K. and Czupyt, Z. 2022. Oxygen isotopes from apatite of Middle and Late Ordovician conodonts in Peri-Baltica (The Holy Cross Mountains, Poland) and their climatic implications. *Geosciences*, **12**, 165, https://doi.org/10.3390/geosciences12040165

Tribovillard, N., Algeo, T.J., Lyons, T. and Riboulleau, A. 2006. Trace metals as paleoredox and paleoproductivity proxies: An update. *Chemical Geology*, **232**, 12–32, https://doi.org/10.1016/j.chemgeo.2006.02.012

Trotter, J.A. and Eggins, S.M. 2006. Chemical systematics of conodont apatite determined by laser ablation ICPMS. *Chemical Geology*, **233**, 196–216, https://doi.org/10.1016/j.chemgeo.2006.03.004

Trotter, J.A., Williams, I.S., Barnes, C.R., Lecuyer, C. and Nicoll, R.S. 2008. Did cooling oceans trigger Ordovician biodiversification? Evidence from conodont thermometry. *Science*, **321**, 550–554, https://doi.org/10.1126/Science.1155814

Trotter, J.A., Williams, I.S., Nicora, A., Mazza, M. and Rigo, M. 2015. Long-term cycles of Triassic climate change: a new δ^{18}O record from conodont apatite. *Earth and Planetary Science Letters*, **415**, 165–174, https://doi.org/10.1016/j.epsl.2015.01.038

Veizer, J. and Prokoph, A. 2015. Temperatures and oxygen isotopic composition of Phanerozoic oceans. *Earth-Science Reviews*, **146**, 92–104, https://doi.org/10.1016/j.earscirev.2015.03.008

Veizer, J., Ala, D. *et al*. 1999. Sr-87/Sr-86, delta C-13 and delta O-18 evolution of Phanerozoic seawater. *Chemical Geology*, **161**, 59–88, https://doi.org/10.1016/S0009-2541(99)00081-9

Veizer, J., Godderis, Y. and Francois, L.M. 2000. Evidence for decoupling of atmospheric CO_2 and global climate during the Phanerozoic eon. *Nature*, **408**, 698–701, https://doi.org/10.1038/35047044

Wallmann, K. 2001. The geological water cycle and the evolution of marine delta O-18 values. *Geochimica Et Cosmochimica Acta*, **65**, 2469–2485, https://doi.org/Doi 10.1016/S0016-7037(01)00603-2

Wang, G.X., Zhan, R.B. and Percival, I.G. 2019. The end-Ordovician mass extinction: a single-pulse event? *Earth-Science Reviews*, **192**, 15–33, https://doi.org/10.1016/j.earscirev.2019.01.023

Wheeley, J.R., Paul Smith, M. and Boomer, I. 2012. Oxygen isotope variability in conodonts: implications for reconstructing palaeozoic palaeoclimates and palaeoceanography. *Journal of the Geological Society*, **169**, 239–250, https://doi.org/10.1144/0016-76492011-048

Yan, D.T., Chen, D.Z., Wang, Q.C. and Wang, J.G. 2012. Predominance of stratified anoxic Yangtze Sea interrupted by short-term oxygenation during the Ordo-Silurian transition. *Chemical Geology*, **291**, 69–78, https://doi.org/10.1016/j.chemgeo.2011.09.015

Yan, D.T., Chen, D.Z., Wang, Q.C., Wang, J.G. and Wang, Z.Z. 2009. Carbon and sulfur isotopic anomalies across the Ordovician-Silurian boundary on the Yangtze Platform, South China. *Palaeogeography Palaeoclimatology Palaeoecology*, **274**, 32–39, https://doi.org/10.1016/j.palaeo.2008.12.016

Yapp, C.J. and Poths, H. 1996. Carbon isotopes in continental weathering environments and variations in ancient atmospheric CO_2 pressure. *Earth and Planetary Science Letters*, **137**, 71–82, https://doi.org/10.1016/0012-821x(95)00213-V

Young, S.A., Saltzman, M.R. and Bergstrom, S.M. 2005. Upper Ordovician (Mohawkian) carbon isotope (delta C-13) stratigraphy in eastern and central North America: Regional expression of a perturbation of the global carbon cycle. *Palaeogeography Palaeoclimatology Palaeoecology*, **222**, 53–76, https://doi.org/10.1016/j.palaeo.2005.03.008

Young, S.A., Saltzman, M.R., Foland, K.A., Linder, J.S. and Kump, L.R. 2009. A major drop in seawater Sr87/Sr86 during the Middle Ordovician (Darriwilian): links to volcanism and climate? *Geology*, **37**, 951–954, https://doi.org/10.1130/G30152a.1

Young, S.A., Saltzman, M.R., Ausich, W.I., Desrochers, A. and Kaljo, D. 2010. Did changes in atmospheric CO_2 coincide with latest Ordovician glacial–interglacial cycles? *Palaeogeography Palaeoclimatology Palaeoecology*, **296**, 376–388, https://doi.org/10.1016/J.Palaeo.2010.02.033

Young, S.A., Gill, B.C., Edwards, C.T., Saltzman, M.R. and Leslie, S.A. 2016. Middle–Late Ordovician (Darriwilian–Sandbian) decoupling of global sulfur and carbon cycles: Isotopic evidence from eastern and southern Laurentia. *Palaeogeography Palaeoclimatology Palaeoecology*, **458**, 118–132, https://doi.org/10.1016/j.palaeo.2015.09.040

Young, S.A., Benayoun, E., Kozik, N.P., Hints, O., Martma, T., Bergstrom, S.M. and Owens, J.D. 2020. Marine redox variability from Baltica during extinction events in the latest Ordovician–early Silurian. *Palaeogeography Palaeoclimatology Palaeoecology*, **554**, https://doi.org/10.1016/j.palaeo.2020.109792

Zhang, L., Cao, L. *et al*. 2017. Raman spectral, elemental, crystallinity, and oxygen-isotope variations in conodont apatite during diagenesis. *Geochimica et Cosmochimica Acta*, **210**, 184–207, https://doi.org/10.1016/j.gca.2017.04.036

Zhang, Y., Tang, P. *et al*. 2021. Climate change in the subtropical Paleo-Tethys before the late Ordovician glaciation. *Global and Planetary Change*, **199**, 103432, https://doi.org/10.1016/j.gloplacha.2021.103432

Zhou, L., Algeo, T.J. *et al*. 2015. Changes in marine productivity and redox conditions during the Late Ordovician Hirnantian glaciation. *Palaeogeography Palaeoclimatology Palaeoecology*, **420**, 223–234, https://doi.org/10.1016/j.palaeo.2014.12.012

Zhang, T.G., Shen, Y.N., Zhan, R.B., Shen, S.Z. and Chen, X. 2009. Large perturbations of the carbon and sulfur cycle associated with the Late Ordovician mass extinction in South China. *Geology*, **37**, 299–302, https://doi.org/10.1130/G25477a.1

Zhang, Y. and Munnecke, A. 2016. Ordovician stable carbon isotope stratigraphy in the Tarim Basin, NW China. *Palaeogeography, Palaeoclimatology, Palaeoecology*, **458**, 154–175, https://doi.org/10.1016/j.palaeo.2015.09.001

Zou, C.N., Qiu, Z. *et al*. 2018. Ocean euxinia and climate change 'double whammy' drove the Late Ordovician mass extinction. *Geology*, **46**, 535–538, https://doi.org/10.1130/G40121.1